1989

Nonlinearity parameters of polymers

Meng-Chou Wu
College of William & Mary - Arts & Sciences

INFORMATION TO USERS

The most advanced technology has been used to photograph and reproduce this manuscript from the microfilm master. UMI films the text directly from the original or copy submitted. Thus, some thesis and dissertation copies are in typewriter face, while others may be from any type of computer printer.

The quality of this reproduction is dependent upon the quality of the copy submitted. Broken or indistinct print, colored or poor quality illustrations and photographs, print bleedthrough, substandard margins, and improper alignment can adversely affect reproduction.

In the unlikely event that the author did not send UMI a complete manuscript and there are missing pages, these will be noted. Also, if unauthorized copyright material had to be removed, a note will indicate the deletion.

Oversize materials (e.g., maps, drawings, charts) are reproduced by sectioning the original, beginning at the upper left-hand corner and continuing from left to right in equal sections with small overlaps. Each original is also photographed in one exposure and is included in reduced form at the back of the book. These are also available as one exposure on a standard 35mm slide or as a 17" x 23" black and white photographic print for an additional charge.

Photographs included in the original manuscript have been reproduced xerographically in this copy. Higher quality 6" x 9" black and white photographic prints are available for any photographs or illustrations appearing in this copy for an additional charge. Contact UMI directly to order.

U·M·I

University Microfilms International
A Bell & Howell Information Company
300 North Zeeb Road, Ann Arbor, MI 48106-1346 USA
313/761-4700 800/521-0600

Order Number 9008532

Nonlinearity parameters of polymers

Wu, Meng-Chou, Ph.D.

The College of William and Mary, 1989

U·M·I

300 N. Zeeb Rd.
Ann Arbor, MI 48106

NONLINEARITY PARAMETERS
OF
POLYMERS

A Dissertation

presented to

The Faculty of the Department of Physics

The College of William and Mary in Virginia

In Partial Fulfillment

of the Requirements for the Degree of

Doctor of Philosophy

---

by

Meng-Chou Wu

1989

APPROVAL SHEET

This dissertation is submitted in partial fulfillment of the requirements for the degree of

Doctor of Philosophy

Author

Approved, May 1989

Joseph S. Heyman, Chairman

William P. Winfree, Co-advisor
NASA Langley Research Center

Harlan E. Schone

William J. Kossler

Gina L. Hoatson

David E. Kranbuehl
Department of Chemistry

To

my grandfather

Arngĩ

and

my grandmother

Hieng

TABLE OF CONTENTS

ACKNOWLEDGEMENTS

I wish to express my gratitude to my advisor, Dr. Joseph S. Heyman for introducing me into this program and his constant encouragement. I am extremely grateful to Dr. William P. Winfree, my advisor at NASA Langley Research Center, for his patiently guiding and caring, his consecutively stimulating and encouraging, in all phases of this research. I am also indebted to Drs. H. E. Schone, W. J. Kossler, G. L. Hoatson, and D. E. Kranbuehl for their carefully reading the manuscript and many valuable criticisms and suggestions; to Dr. W. T. Yost for his guidance of lapping samples; and to Messrs. F. R. Parker, F. D. Stone, and C. G. Clendenin for their technical assistance.

I am deeply grateful to my parents for their constant understanding and sacrifice; also to my sisters and brothers for their sharing my responsibility to the family. Pursuing the higher education would be otherwise impossible for me. Having come to this country, enduring the poor student-life, bearing the recurring sorrow, my wife, Wen-Shu and my daughters, Yi-Chen and Yi-Heng deserve the honor, if I can say some words about my complement.

LIST OF TABLES

LIST OF FIGURES

ABSTRACT

Three types of acoustic nonlinearity parameters for solids are discussed. The results of measurements of these parameters for three polymers—polymethyl methacrylate, Polystyrene, and polysulfone—are presented.

The author has developed a new technique, using piezoelectric transducers directly bonded to the specimens, which allows the measurements of fundamental and second harmonics generated in the solids, and thereby the determination of nonlinearity parameter β_3, which is the ratio of a linear combination of second- and third-order elastic coefficients to the second-order elastic coefficient.

The second nonlinearity parameter, B/A can be determined from the temperature and pressure derivatives of the sound velocity. We derive its exact relationship for the case of solids. The results from the two techniques are shown to be consistent.

The pressure derivative of the sound velocity is also related to the Grüneisen parameter, which can be used to describe the anharmonicity of interactions in polymer molecules, especially of interchain vibrations. The interchain specific heat for these polymers is then calculated from the Grüneisen parameters; and the characterization of polymers by using these thermoacoustic parameters is discussed.

NONLINEARITY PARAMETERS

OF

POLYMERS

I. INTRODUCTION

A consideration of nonlinearity is essential for describing many important physical phenomena and processes in solids. The phenomena which are dominated by the nonlinear contributions can be sorted into two groups [Ashcroft 1976]. First, equilibrium properties: thermal expansion, the most important one; the temperature and pressure dependence of elastic constants; and the difference between adiabatic and isothermal elastic constants (or other thermal constants). Secondly, transport properties: the finiteness of the thermal conductivity of a solid (a purely harmonic theory would lead to an infinite thermal conductivity); also, the processes by which, for example, the lattice vibrations transmit energy.

Since nonlinearity accounts for various physical phenomena, there are, as well, various "nonlinearity parameters," defined according to their specific relationships with physical quantities in their respective conditions. For example, the Grüneisen constants, originally from the theory of Debye solids; the temperature and pressure coefficients

of elastic constants; the nonlinearity parameter from harmonic generation. These nonlinearity parameters represent different aspects of nonlinear properties of solids; and of course, can be related to each other.

The nonlinearity parameter from harmonic generation, denoted β_3 here, is a well-known and widely used physical constant for characterizing the nonlinear properties of solids [Wallace 1970]. When a longitudinal, sinusoidal acoustic wave of a given fundamental frequency is traveling through a medium, its second and higher harmonics are generated. The amplitude of the second harmonic is proportional to both the nonlinearity parameter and the squared amplitude of the fundamental. Measurements of the amplitudes of the fundamental and the second harmonic are used to obtain β_3, which is actually the ratio of a linear combination of second- and third-order elastic constants to the second-order elastic constant. Conventionally, a capacitive detector is used to measure the absolute displacements of the fundamental and the harmonic [Gauster 1966].

In this research we use a new technique to measure the nonlinearity parameter. Recently Wu and Winfree [1987] have developed a physical model of piezoelectric measurement system, which allows the measurements of the fundamental and the second harmonic displacement. The primary application of

this technique is for measuring the nonlinearity of polymers which is the focus of this research.

Polymers, as crystals or glasses, are distinguished from other solids in two respects. First, they contain long-chains of molecules, in which the repeating unit generally still consists of several atoms. Second, the molecular interaction in a polymer is strongly anisotropic, that is, the basic units are combined by strong covalent bonds along the chain axis, while by relatively weak van der Waals forces perpendicular to the chain.

Concerning the molecular motions of polymers, let us ignore the less important intra-unit vibrations and discuss mainly the skeleton or chain vibrations. [Wada 1969] The skeleton vibrations consists two types: interchain (chain-to-chain) vibrations which are essentially governed by van der Waals forces between the chains; and intrachain (within-a-chain) vibrations governed by covalent forces. Obviously the covalent bond has a force constant much larger than the van der Waals bond; therefore, as far as the high frequency (typically higher than 10^{12} Hz [Barker 1967]) or short wavelength modes of vibrations are concerned, the intrachain vibrations dominate and the interchain potential can be ignored to a good approximation. Therefore, one can model the polymer as an assembly of isolated one dimensional

chains. As for low frequency vibrations, the contribution of interchain potential becomes comparable to, or even larger than, that of the intrachain potential. Apparently, there is no clear frequency band that sorts out the two classes of vibrations; modes wax and wane continuously as the frequency changes.

Nevertheless, the nonlinear properties of polymers are closely related to the interchain potential. It is of interest that the interchain vibrations exhibit great anharmonicity while the intrachain vibrations show much less, or none. [Swan, 1962] The measurement of nonlinearity parameter, therefore, may be only sensitive to the interchain vibrations. As a result, it is possible to determine the contribution of the interchain interactions to some physical quantities. For example, there are two types of Grüneisen parameters, as described in section 2.3. [Slater 1939] One is calculated from thermal expansion, bulk modulus, and specific heat. This is the macroscopic, or thermodynamic, Grüneisen parameter which is a result of an average over all modes of vibrations. The other one is determined by using the pressure dependence of the ultrasonic velocity. Only the interchain vibrations contribute to this acoustic Grüneisen parameter. By comparing the values of two different Grüneisen parameters, the heat capacity from the interchain vibrations then can be estimated.

The purpose of this research is the following: (1) To develop a new technique for measuring β_3. The author has developed a physical model of piezoelectric measurement system, allowing the determination of fundamental and second harmonic absolute amplitudes and therefore β_3. This technique has made possible the first acoustic measurement of the nonlinearity of polymers. (2) To derive an exact relationship for determining the second nonlinearity parameter, B/A, from the temperature and pressure dependence of the ultrasonic velocity. B/A is widely used for characterizing fluids. However, for the case of solids, A relationship between B/A and the acoustic measurable quantities was not available. This has led to some confusion in the literature. We derive an exact relationship which, combined with acoustic measurements, gives results consistent with those from the first technique, thus resolving the confusion. (3) To relate the ultrasonic nonlinearity parameters of polymers to their thermodynamic properties. (4) To relate the pressure derivative of the sound velocity to the Grüneisen parameter, which is used to described the anharmonicity of the interchain interactions in polymers.

In chapter II we start from the nonlinear wave equation to describe the harmonic generation and show how β_3 can be obtained. Then we discuss B/A and derive its exact relationship with the temperature and pressure coefficients of ultrasonic velocities for solids. We also show how the

pressure coefficient of the ultrasonic velocity can be used to calculate the Grüneisen parameter; and compare the latter with the thermodynamic Grüneisen parameter. Chapter III focuses on a description of the basic ultrasonic techniques and equipment used in this research. Also the general properties and preparation processes of three investigated polymers—polymethyl methacrylate, polystyrene, and polysulfone—are described. Chapter IV is a demonstration of a physical model of piezoelectric transducers and a new technique for measuring the acoustic displacement by using this model. To test the model, the fundamental displacement measurements for several metals are presented. In Chapter V, we describe the experimental procedures of measuring β_3 for polymers using the technique mentioned above; and discuss the attenuation correction for the calculation of β_3. In addition, we discuss the measurements of temperature and pressure dependence of ultrasonic velocity and show how the velocity is obtained from measurements of the ultrasonic transit time. In Chapter VI the experimental results are analyzed and the values of various nonlinearity parameters for three polymers are presented. Also calculated are the Grüneisen parameters and interchain specific heat for these polymers. Finally, we discuss using these nonlinearity parameters for the characterization of interchain interactions in polymers.

II. NONLINEAR THEORY OF SOLIDS

2.1 The Nonlinear Equation of Motion and the Nonlinearity Parameter β_3

The general equation of motion for a longitudinal wave propagating in a nonlinear elastic solid can be written as [Thurston 1967, Wallace 1970]

$$\rho_0 \ddot{u}_i = \partial_k \partial_l u_j (M_{ikjl} + \partial_q u_p M_{ikjlpq} + \cdots), \qquad (2.1.1)$$

where u_i are the displacement components, $\partial_k \equiv \partial/\partial x_k$, x_k denote the Lagrangian coordinates; and

$$M_{ikjl} = c_{ikjl},$$

$$M_{ikjlpq} = c_{ikjlpq} + \delta_{jp} c_{iklq} + \delta_{ij} c_{klpq} + \delta_{ip} c_{kjlq};$$

where c_{ikjl} and c_{ikjlpq} are second- and third-order adiabatic (isentropic) elastic constants respectively. (Note that the Einstein summation convention is adopted: a repeated suffix denotes a summation over the values 1 to 3.)

For one-dimensional motion in an isotropic solid, the equation can be reduced to the form

$$\rho_0 \ddot{u} = \frac{\partial^2 u}{\partial x^2}\left[M_2 + M_3 \frac{\partial u}{\partial x} + \cdots\right], \tag{2.1.2}$$

where x is the coordinate in the direction of propagation, M_2 a linear combination of second-order elastic coefficients, and M_3 a linear combination of second- and third-order coefficients. In the literature M_3 is sometimes expressed as

$$M_3 = K_3 + 3K_2,$$

where $K_2 \equiv M_2$ and K_3 the third order elastic constant.

Assume a steady driving term such that, for a semi-infinite solid at $x = 0$, $u = A_0 g(t)$, where $g(t)$ is typically a tone burst, defined to have a maximum amplitude of 1, and A_0, the displacement, is very small compared to the wavelength λ. With this assumption a method of iteration, i.e., successive approximations for solutions to the fundamental and harmonic waves can be used to solve (2.1.2). [Thompson 1977]

For the first order approximation the Eq. (2.1.2) can be rewritten as

$$\ddot{u} - c^2 \frac{\partial^2 u}{\partial x^2} = c^2 \frac{\partial}{\partial x}\left[\frac{\beta_3}{2}\left(\frac{\partial u}{\partial x}\right)^2\right], \tag{2.1.3}$$

where c is the infinitesimal amplitude sound velocity with $c^2 = M_2/\rho_0$ and the nonlinearity of the solid is characterized by β_3, which is defined by

$$\beta_3 \equiv M_3/M_2. \tag{2.1.4}$$

Obviously the zeroth order solution has the form of a traveling wave, $u_0(x,t) = A_0 g(t - x/c)$. By substituting this zeroth order solution into the quadratic term on the right-hand side of Eq. (2.1.3), the first order solution can be obtained as

$$u_1(x,t) = A_0 g(t - x/c) + \frac{1}{4} x \beta_3 A_0^2 \left[\frac{\partial g(t - x/c)}{\partial x}\right]^2. \tag{2.1.5}$$

The first term in the solution has the same form as the traveling wave and is referred to as the fundamental. The second term, which is the result of the nonlinearity of the solid (characterized by β_3), is generated by the fundamental and increases linearly as the wave propagates through the

solid.

The measurement of the acoustic wave is made at a single plane in the solid and evaluated as a function of time. It is convenient to convert the derivative in Eq. (2.1.5) into a time derivative for applying the equation to a real measurement. For any propagating function $g(t - x/c)$, $\partial g/\partial x = -(1/c)(\partial g/\partial t)$. The solution (2.1.5), therefore, can be expressed as

$$u(x,t) = A_0 g(t - x/c) + \frac{1}{4c^2} x \beta_3 A_0^2 \left[\frac{\partial g(t - x/c)}{\partial t}\right]^2 \qquad (2.1.6)$$

(with subscript 1, which denotes the first order solution, dropped). The shape of the wave recorded as a function of time can be used then to infer the magnitude of the nonlinearity.

For a continuous sinusoidal excitation, $g(t - x/c)$ in (2.1.6) is replaced by $\cos(\omega t - x/c)$, then

$$[\partial \cos(\omega t - kx)/\partial t]^2 = \omega^2 \sin^2(\omega t - kx)$$

$$= \frac{1}{2}\omega^2 [1 - \cos 2(\omega t - kx)].$$

The nonlinear term of (2.1.6) can be written as

$$(x\beta_3 A_0^2 k^2/8)[1 - \cos 2(\omega t - kx)],$$

where the first term is the static displacement and the second term is the second harmonic. To determine the nonlinearity parameter, measurements are made by comparing either the static displacement [Li, 1984] or the second harmonic amplitude to the amplitude of the fundamental, This research concentrates on the latter.

2.2 Another Nonlinearity Parameter B/A

In the previous section, we have described the nonlinearity for longitudinal waves propagating in solids. It is of interest to note that nondissipative fluids are governed by an equation of motion which has the same form as that for solids. A considerable amount of work for the nonlinearity of fluids has been done [Beyer 1965]. The analysis of some cases can apply directly to the solids with an appropriate choice of the parameters.

Let x_i denote the Cartesian coordinates of a particle in the unstressed reference configuration and $y_i(x_i,t)$ the coordinates of the same particle in an arbitrary configu-

ration. For a nondissipative solid, the stress is T_{ij}, the general equation of motion has the form

$$\rho\ddot{u}_j = \partial T_{ij}/\partial y_i, \tag{2.2.1}$$

which can be expressed as

$$\rho\ddot{u}_j = (\partial x_i/\partial y_j)(\partial T_{ij}/\partial x_i). \tag{2.2.2}$$

It is convenient to define a Jacobian J to indicate the geometry of strain:

$$J \equiv \det[\partial y_i/\partial x_j] = \rho_0/\rho. \tag{2.2.3}$$

By substituting (2.2.3) into (2.2.2), the equation of motion is transformed to

$$\rho_0\ddot{u}_j = J(\partial x_i/\partial y_j)(\partial T_{ij}/\partial x_i). \tag{2.2.4}$$

For one-dimensional, purely longitudinal motion in the direction along the coordinate x, the Jacobian becomes

$$J = \rho_0/\rho = \partial y/\partial x = 1 + (\partial u/\partial x), \tag{2.2.5}$$

with all subscripts dropped; and let

$$p_1 \equiv -T_{xx}, \tag{2.2.6}$$

parameterize the longitudinal stress. By using Eqs. (2.2.4) and (2.2.5), a one-dimensional equation of motion can be written as

$$\rho_0 \ddot{u} = -(\partial p_1/\partial x). \tag{2.2.7}$$

By assuming the longitudinal stress is a function of the density such that

$$\frac{\partial p_1}{\partial x} = \frac{dp_1}{d\rho}\frac{\partial \rho}{\partial x} = -\frac{\rho^2}{\rho_0}\frac{dp_1}{d\rho}\frac{\partial}{\partial x}\left(\frac{\rho_0}{\rho}\right) = -\frac{\rho^2}{\rho_0}\frac{dp_1}{d\rho}\frac{\partial^2 u}{\partial x^2}. \tag{2.2.8}$$

Eq.(2.2.7) is then expressed as

$$\ddot{u} = -\left(\frac{\rho^2}{\rho_0^2}\frac{dp_1}{d\rho}\right)\frac{\partial^2 u}{\partial x^2}. \tag{2.2.9}$$

The coefficient of the second derivative on the right-hand side of Eq. (2.2.9) is corresponding to that of Eq.(2.1.1).

The relation between p_1 and ρ can be described by using the Taylor expansion

$$p_1 = p_0 + A\xi + \frac{1}{2} B\xi^2 + \cdots \tag{2.2.10}$$

where

$$\xi \equiv (\rho - \rho_0)/\rho_0 = J^{-1} - 1 = -J^{-1}(\partial u/\partial x), \tag{2.2.11}$$

$$A = \rho_0(\partial p_1/\partial \rho)_{S,\ \rho=\rho_0}, \tag{2.2.12}$$

and

$$B = \rho_0^2(\partial^2 p_1/\partial \rho^2)_{S,\ \rho=\rho_0}. \tag{2.2.13}$$

With this notation, the factor inside the brackets of Eq. (2.2.9) can be written as

$$\frac{\rho^2}{\rho_0^2}\frac{\partial p_1}{\partial \rho} = \frac{J^{-2}}{\rho_0}(A + B\xi + \cdots). \tag{2.2.14}$$

By applying the binomial theorem to each negative power of J, (2.2.14) can be expanded as a power series in $\partial u/\partial x$. The equation of motion thereby becomes

$$\ddot{u} = \frac{A}{\rho_0}\frac{\partial^2 u}{\partial x^2}\left[1 - \left(2 + \frac{B}{A}\right)\frac{\partial u}{\partial x} + \cdots\right]. \tag{2.2.15}$$

and B/A defines the nonlinearity of the solid. A comparison of this expression and the equation of motion (2.1.2) in section 2.1 gives the relationship between this and the pre-

viously defined nonlinearity parameter as

$$\beta_3 \equiv \frac{M_3}{M_2} = -\left(2 + \frac{B}{A}\right), \tag{2.2.16}$$

For the case of zero shear modulus, i.e., fluids, B/A is simply the pressure derivative of the bulk modulus, and can be calculated from the pressure derivative of the ultrasonic velocity. However, for the case of solids, B/A is no longer simply the pressure derivative of the bulk modulus. This has led to some confusion in the literature. In the following, we derive the exact relationship between B/A and thermo-acoustic properties for solids.

In general, the stress tensor can be expressed in terms of the strain tensor for an isotropic body [Landau 1959] as

$$T_{ik} = B_S u_{jj}\delta_{ik} + 2\mu(u_{ik} - \tfrac{1}{3}u_{jj}\delta_{ik}), \tag{2.2.17}$$

where T_{ik} is the stress tensor, u_{ik} the strain tensor, δ_{ik} the unit tensor ($\delta_{ii} = 3$), B_s the adiabatic bulk modulus, μ the shear modulus. Therefore, for one-dimensional, purely longitudinal motion, the stress is expressed as

$$T_{xx} = (B_S + \tfrac{4}{3}\mu)u_{xx} = M_2 u_{xx} = -p_1 . \tag{2.2.18}$$

For small deformations, u_{xx} (the only relative volume change) and p_1 are small quantities, the ratio u_{xx}/p_1 of the relative volume change to the longitudinal stress can be written in the differential form $(1/V)(\partial V/\partial p_1)_S$. Thus the expression (2.2.12) becomes

$$A = -V_0 \left(\frac{\partial p_1}{\partial V}\right)_{S,V=V_0} = M_2 . \tag{2.2.19}$$

Since the expression (2.2.13) can be also written as $B = V_0^2(\partial^2 p_1/\partial V^2)_{S,V=V_0}$, by using (2.2.19), the nonlinearity parameter B/A can be expressed as

$$\begin{aligned} \frac{B}{A} &= \frac{V_0^2 \dfrac{\partial}{\partial V}\left(-\dfrac{M_2}{V_0}\right)_{S,V=V_0}}{M_2} \\ &= -\frac{V_0}{M_2}\left(\frac{\partial M_2}{\partial p}\right)_S \left(\frac{\partial p}{\partial V}\right)_{S,V=V_0} \end{aligned} \tag{2.2.20}$$

Note that in (2.2.20) there is a change in variable from volume V to isotropic pressure p for the derivative. Thereby the nonlinearity parameter B/A is related to the pressure dependence of the longitudinal modulus. For the bulk modulus $B_S = -V(\partial p/\partial V)_S$, Eq. (2.2.20) becomes

$$\frac{B}{A} = \frac{B_S}{M_2}\left(\frac{\partial M_2}{\partial p}\right)_S \tag{2.2.21}$$

For the case of fluids ($B_S = M_2$), this reduce to $B/A = (\partial B_S/\partial p)_S$.

A value for B/A can be obtained by various methods, including ultrasonic measurement by using (2.2.21). Through a thermodynamic transformation and substitution of c_1^2/V for M_2, the isentropic derivative in (2.2.21) can be written as

$$\left(\frac{\partial M_2}{\partial p}\right)_S = \left(\frac{\partial M_2}{\partial p}\right)_T + \frac{\alpha V T}{C_p}\left(\frac{\partial M_2}{\partial T}\right)_p$$
$$= \frac{2c_1^2}{V}\left(\frac{\partial \ln c_1}{\partial p}\right)_T + \frac{2c_1^2 \alpha T}{C_p}\left(\frac{\partial \ln c_1}{\partial T}\right)_p \qquad (2.2.22)$$

where c_1 is the longitudinal velocity, C_p the specific heat at constant pressure, and $\alpha = (\partial \ln V/\partial T)_p$, the volume coefficient of expansion. The relative changes of the ultrasonic velocity with respect to pressure and temperature are:

$$K_T \equiv -\left(\frac{\partial \ln c_1}{\partial \ln V}\right)_T = \frac{1}{\beta_T}\left(\frac{\partial \ln c_1}{\partial p}\right)_T \qquad (2.2.23)$$

and

$$K_p \equiv -\left(\frac{\partial \ln c_1}{\partial \ln V}\right)_p = -\frac{1}{\alpha}\left(\frac{\partial \ln c_1}{\partial T}\right)_p \qquad (2.2.24)$$

where $\beta_T = 1/B_T = -(\partial \ln V/\partial p)_T$, is the isothermal compressibility. Then (2.2.22) becomes

$$\left(\frac{\partial M_2}{\partial p}\right)_S = 2M_2\left[\beta_T K_T - \frac{\alpha^2 VT}{C_p} K_p\right] \tag{2.2.25}$$

Using this expression and the well known thermodynamics relations

$$C_p - C_V = \alpha^2 VT/\beta_T \tag{2.2.26}$$

and

$$\gamma \equiv C_p/C_V = B_S/B_T = \beta_T/\beta_S, \tag{2.2.27}$$

expression (2.2.21) becomes

$$\begin{aligned}\frac{B}{A} &= 2\left[B_S\beta_T K_T - B_S\beta_T\left(\frac{C_p - C_V}{C_p}\right)K_p\right] \\ &= 2[\gamma K_T - (\gamma - 1)K_p] \\ &= 2[K_T + (\gamma - 1)(K_T - K_p)]\end{aligned} \tag{2.2.28}$$

Therefore the nonlinearity parameter B/A for a solid is derivable from measurements of the pressure and the temperature coefficients of the acoustic velocity, and some thermal constants. Since γ is approximately equal to 1 and K_T is of

the same order as K_p, $(\gamma - 1)(K_T - K_p)$ in (2.2.28) is then relatively small; therefore, $B/A \approx 2K_T$, and to the first order the pressure coefficient of the acoustic velocity is all that is required for determining the nonlinearity parameter.

2.3 Grüneisen Parameters and Interchain Interactions

The Grüneisen parameter is the third nonlinearity parameter, classically used to characterize the nonlinear properties of solids. Its original definition is based on the Debye model of phonon spectrum. Although, Debye model is a rough approximation, it is nevertheless an effective approach for investigating some nonlinear properties, such as thermal expansion, of solids. According to Debye's theory, the frequency spectrum is characterized by the limiting frequency ω_{max}, and if this frequency changes, all other oscillations change their frequencies in the same ratio. [Slater 1939] This frequency is sometimes called Debye frequency and can be expressed as

$$\omega_D = c_s(6\pi^2 N/V)^{1/3}, \qquad (2.3.1)$$

where N is the number of oscillators per unit mass and c_s the effective, or average sound velocity for the Debye

solid, defined by the relation [Reif 1965]

$$\frac{1}{c_s^3} \equiv \frac{1}{c_l^3} + \frac{2}{c_t^3}. \tag{2.3.2}$$

The form of the weighted average comes from the fact that, in general, a sound wave includes the longitudinal mode with single component and the shear mode with two components.

A Grüneisen parameter for each oscillator with frequency ω_i is defined as

$$\Gamma_i \equiv - \frac{d\ln\omega_i}{d\ln V}. \tag{2.3.3}$$

In the Debye model, all the normal-mode frequencies scale linearly with the cutoff frequency ω_D; therefore, it implies the Grüneisen's assumption that Γ_i is the same for all frequencies and equals to an overall Grüneisen parameter,

$$\Gamma = - \frac{d\ln \omega_D}{d\ln V}. \tag{2.3.4}$$

From Eq. (2.3.1) it can be shown

$$\ln\omega_D = \ln c_s - \frac{1}{3}\ln V + \text{const.} \tag{2.3.5}$$

and therefore

$$\Gamma = -\frac{d\ln c_s}{d\ln V} + \frac{1}{3}. \tag{2.3.6}$$

Eq. (2.3.6) means that one can find the Grüneisen parameter from measurable acoustical quantities. For a isothermal process, (2.3.6) becomes

$$\Gamma_T = -\left(\frac{\partial \ln c_s}{\partial \ln V}\right)_T + \frac{1}{3}. \tag{2.3.6a}$$

or

$$\Gamma_T = \frac{1}{\beta_T}\left(\frac{\partial \ln c_s}{\partial p}\right)_T + \frac{1}{3} \tag{2.3.6b}$$

From the same (Grüneisen's) assumption, by relating the heat capacity and the thermal expansion, an expression for Γ in terms of the thermodynamic properties of the solid is given as [Slater 1939]

$$\Gamma = \frac{\alpha V}{\beta_T C_V}. \tag{2.3.7}$$

This is sometimes seen as a thermodynamic definition of the Grüneisen parameter, and is an average over all the vibrational modes. Thus, besides using expression (2.3.6), one can also use measured values of thermal expansion, compressibility, specific heat, and volume to determine empirical values of Γ.

In general the results from the two methods (Eq.(2.3.6b) and Eq.(2.3.7)) of finding Γ are not necessarily the same. For most metals and ionic crystals, the agreement between the two methods is within an order of magnitude ($\Gamma \approx \Gamma_T$), with the values between 1 and 3, typically on the order of 2. However, for polymers the difference becomes significantly large, with Γ_T 5 to 10 times the value of Γ [Warfield 1974, Hartmann 1976]. As we mentioned in Chapter I, the molecular interaction in a polymer is highly anisotropic. Interchain vibrations, which involve van der Waals forces, are low frequency and anharmonic, and have high Grüneisen values; while intrachain vibrations, which involve covalent bonds, are high frequency and harmonic, and have very low Grüneisen values. Γ is determined by various dynamic techniques and is a result of an average over all modes of the vibrations. In contrast, by using acoustic techniques, Γ_T is dominated by interchain vibrations since all the ultrasonic waves are relatively low-frequency.

An important assumption is that only interchain vibrations of polymer solids exhibit anharmonicity. It has been shown [Swan 1962] that the thermal expansion of polymer crystals is much smaller along the chain axis than in the plane perpendicular to the axis. Therefore, for polymers, only the portion of the specific heat due to the interchain vibrations, $C_{V,i}$ should be include in (2.3.7) [Wada 1969], resulting in a definition for $C_{V,i}$,

$$C_{V,i} = \frac{\alpha V}{\beta_T \Gamma_T}. \qquad (2.3.8)$$

Therefore, using ultrasonics with thermodynamic measurements, one is able to separate the contributions of inter- and intra-chain interactions to the heat capacity.

III. EQUIPMENT AND SAMPLES

3.1 The Basic Equipment for the Velocity Measurement

The measurement of sound velocity is the basis of the acoustical investigation of materials. Many different methods with different degrees of accuracy have been developed. The basic pulse-echo method is a generally used technique. A gated rf signal of a given frequency is applied to a piezoelectric transducer and thereby converted into a pulsed ultrasonic wave of the same frequency. The pulsed wave travels through the specimen and is reflected between two end surfaces of the specimen until it decays away. The ultrasonic wave velocity propagating in the specimen can then be determined by measuring the transit time between the echoes and the corresponding propagation distance.

A straightforward method to measure velocities is to pick any pair of echoes and measure the time interval between corresponding wave reference points such as their leading edges. However, each time the pulse hits the bonded end, the specimen-bond-transducer interface introduces a

phase shift to the reflected wave. These phase shifts make the determination of reference points difficult and limit the accuracy of the method. To resolve this problem, many other methods [Papadakis, 1976; Breazeale, 1981] have been developed: pulse superposition, double-pulse, echo-overlap, and so forth. All of them involve sophisticated electronic circuitry and have a common feature: matching full range of echoes and then removing the phase shift so that a more accurate transit time can be obtained.

Modern digitizers can digitize signals and transfer them to computers for off-line processing and analysis. For example, cycle-for-cycle matching of the echoes can then be done by curve-fitting the digitized wave forms with a computer program. This technique reaches similar accuracy and precision as those refined pulse-echo methods with reduced human interaction and interpretation.

A block-diagram of the experimental setup used in this study is shown in Fig. 3.1.

A Pulse/Function Generator is used to generate the gated rf bursts. A suitable length of the output sinusoidal wave, counted by cycles, can be chosen to meet the various measurement conditions of the specimens.

A solid state 40W amplifier (with a linear gain in the range of 20kHz to 10Mhz) is used to amplify the rf burst. To protect the input amplifier of the digitizer during the drive pulse and decouple the output noise of the amplifier from the receiver, a diode box couples the amplifier, the transducer, and the digitizer.

The resulting waveforms from the output of the transducer are recorded by a digitizer with a bandwidth from DC to 125MHz at 50Ω. To increase the signal to noise ratio, the waveforms are averaged in the digitizer before being transferred to a computer to be post-processed and archived.

To obtain a pulse-echo pattern, one transducer is bonded to the specimen. When the attenuation of the specimen is too high, two transducers are used and through-transmission (sometimes, called pitch-catch) measurements are taken. This method is especially suitable for measuring relative changes of velocity.

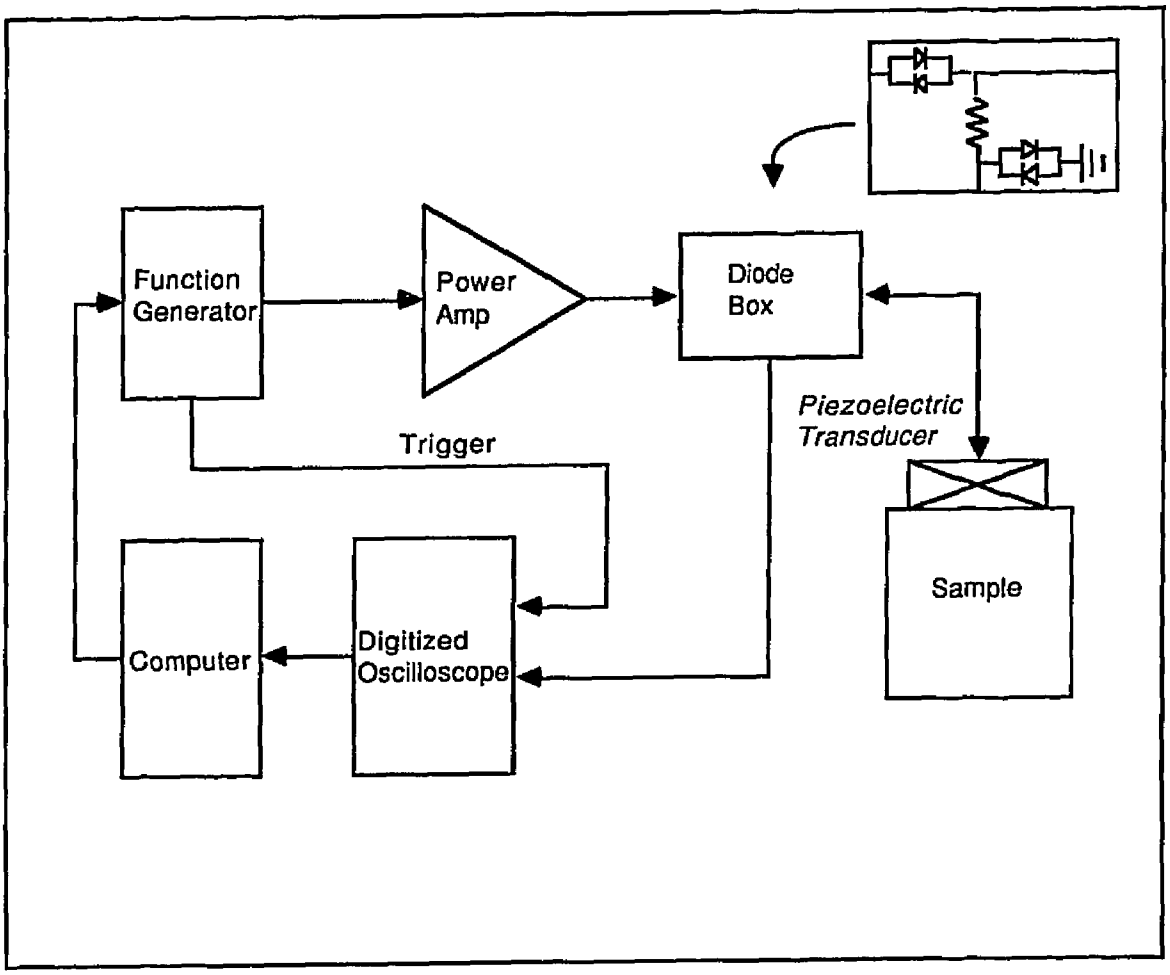

Fig. 3.1 Block diagram of the velocity measurement.

3.2 The Temperature Controller and the Pressure System

For measuring the temperature dependence of the ultrasonic velocity or keeping the specimen in an isothermal condition, a high precision temperature controller was built. This has an insulated box containing an interior aluminum chamber with a resistor of about 50Ω as a heater, which is driven by the output of a computer-controlled function generator. A thermocouple attached to the specimen determines the temperature, which is recorded by a computer. The computer also determines the power output to the resistor required to maintain a constant temperature. The power is adjusted about every half minute. This system controls the temperature to within ±0.02°C for a range from room temperature to 70°C. A block diagram of the apparatus and arrangement is shown in Fig. 3.2.

For measuring the pressure dependence of velocities, the pressure system shown schematically in Fig. 3.3 is used. The specimen is inserted in a brass chamber surrounded by a heater. The chamber is placed in the pressure vessel, which receives a gas-intake of 0-250psi. A bourdon gauge and a digital pressure gauge are used to monitor the pressure to 0.1 psi. The temperature was isothermally controlled by a commercial temperature controller with fluctuation less than 0.05°C.

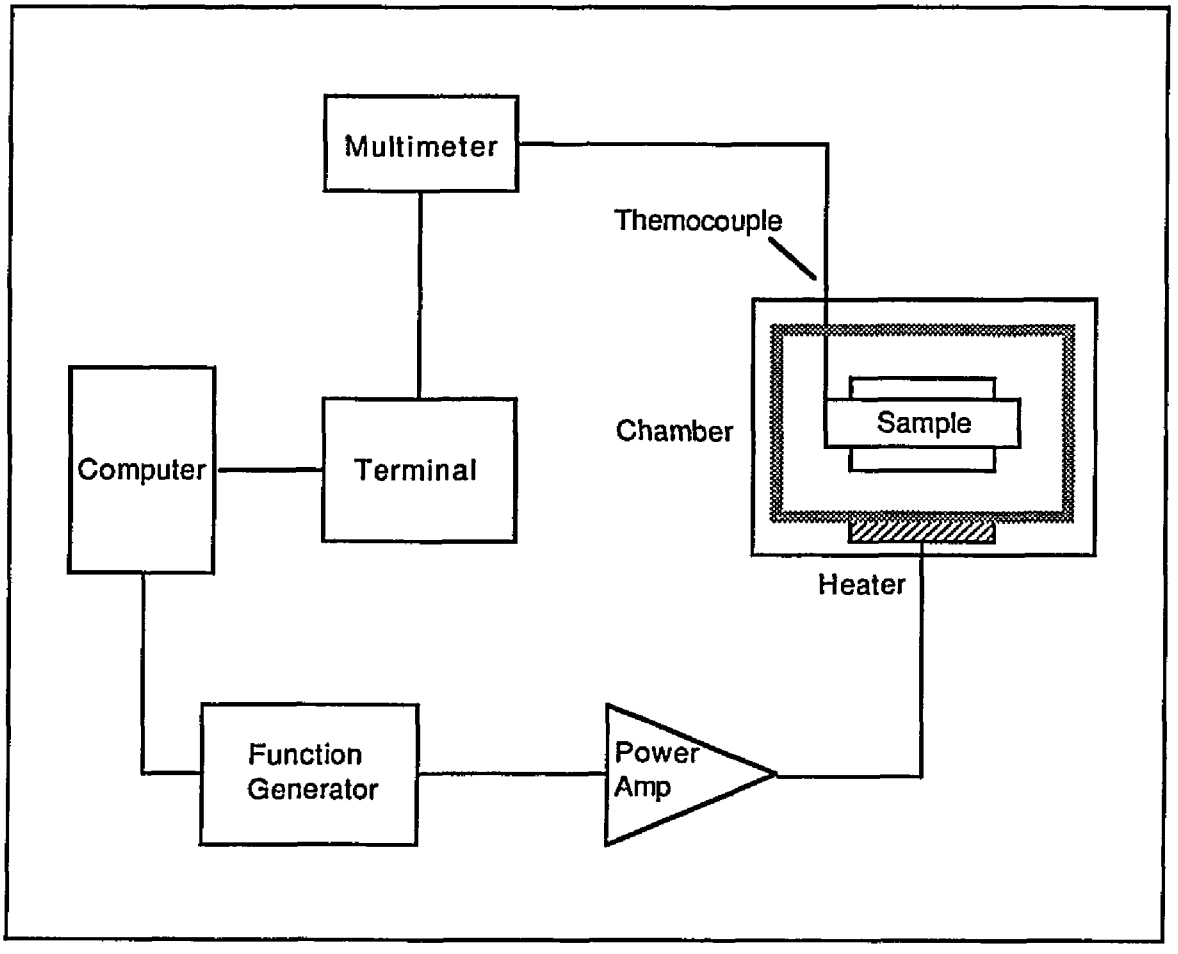

Fig. 3.2 Block diagram of the temperature controller for measuring the temperature coefficient of ultrasonic velocity.

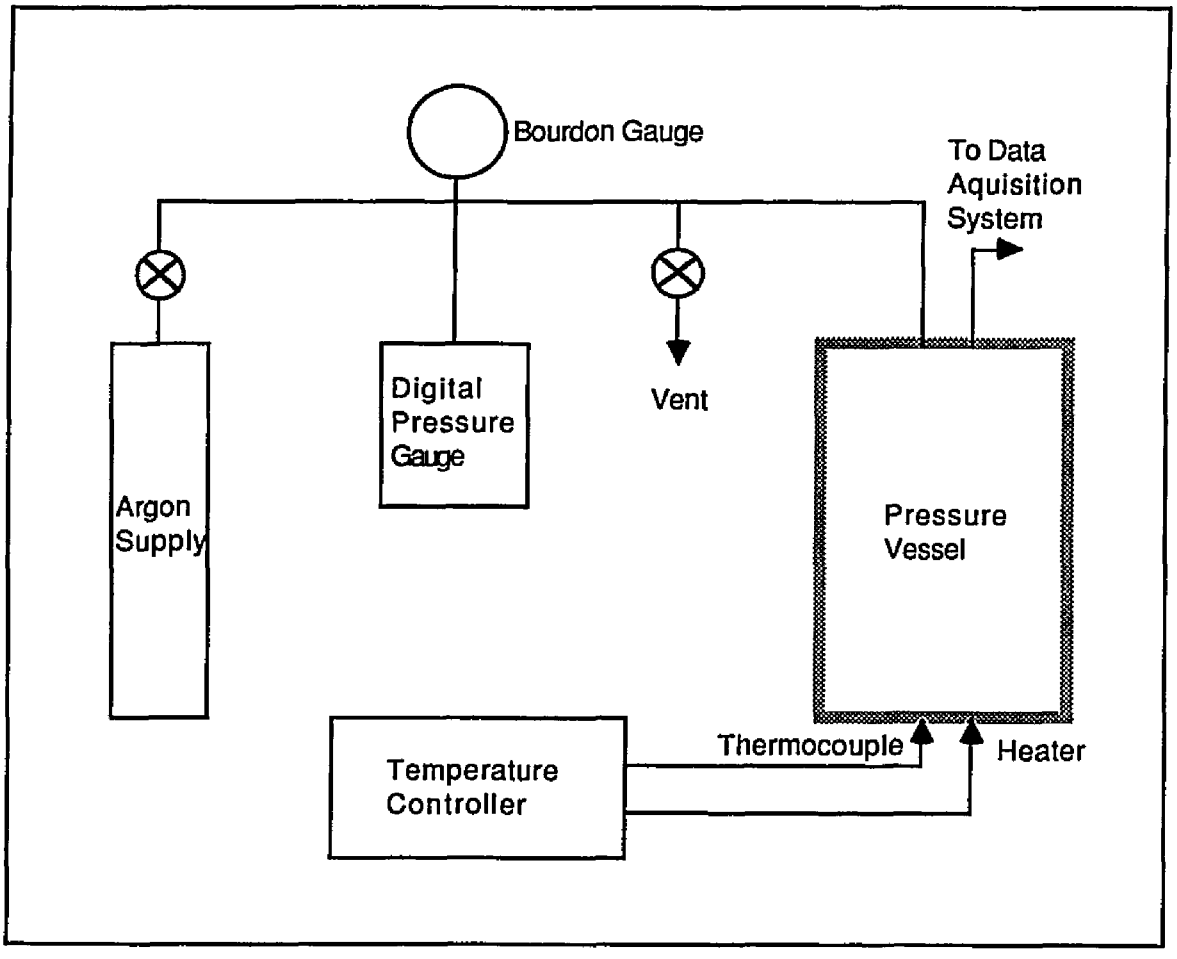

Fig. 3.3 Block diagram of the pressure system for measuring the pressure coefficient of ultrasonic velocity.

3.3 Samples and Sample preparation

Three amorphous polymers, polymethyl methacrylate (PMMA), polystyrene (PS), and polysulfone (PSF) are used for specimens in this work. PMMA and polystyrene are the most extensively studied polymeric materials [Asay 1969, Lamberson 1972]. Polysulfone is a widely used and studied polymer for its high rigidity and strength, and, especially its high temperature thermoplastic properties [Phillips 1977, Allen 1971].

The molecular structures of these polymers are shown in Table 3.1 The samples were obtained from commercial products as a form of cast rod (PMMA and Polystyrene) or beads (PSF, Udel-1700).

The glass transition temperature for each of these polymers was determined by using an ultrasonic technique [Parker 1986]. The results are given in Table 3.2.

The specimens for all measurements were molded into disks, 3.8cm in diameter and of various thicknesses at a temperature about 30-40°C above T_g and a pressure of about 4000 psi for each polymer. The samples were left in the molder and cooled slowly to release thermal stress. After cooling off, the samples were then lapped until they

exhibited flatness on the order of 1μm and parallelism of less than 10 sec of arc.

The density of each material was obtained by weighing the specimens and measuring their physical dimensions. The average density of each polymer is shown in Table 3.2.

A thin aluminum layer of about 1000Å thickness was then deposited on one or both flat sides of each finished specimen for the different demands of various measurements.

TABLE 3.1

The Molecular Structures of Three Investigated Polymers

Polymethyl methacrylate (PMMA)

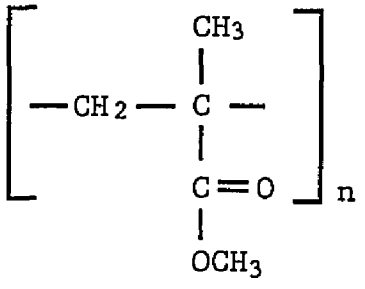

Polystyrene (PS)

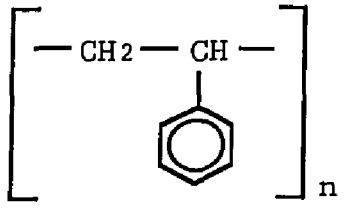

Polysulfone (PSF)

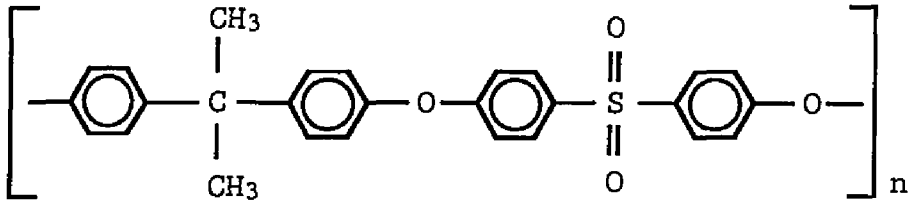

TABLE 3.2

The Density and Glass Transition Temperature of Three Polymers

	PMMA	PS	PSF
ρ (kg/m^3)	1186	1050	1236
T_g (°C)*	105	100	183

*The determination of T_g is at a heating rate of 2°C/min.

IV. ABSOLUTE DISPLACEMENT MEASUREMENTS WITH PIEZOELECTRIC TRANSDUCERS

Absolute displacement measurements are required for measurements of ultrasonic nonlinearity in a solid, to determine amplitudes of the fundamental and harmonic waves. Typically such measurements are made by a parallel plate capacitive detector with narrow gap spacing [Gauster 1966] between an external electrode and one side of the specimen. By measuring the capacitance of the gap and the bias voltage on the electrode, it is possible to calculate the absolute displacement of the surface of the sample as a function of time from the output signal of the capacitive detector [Li, 1984].

For appreciable signals from the capacitive transducer, the area of the surfaces forming the capacitor must be approximately 1 cm^2 and the gap spacing less than 10 μm. This requires the sample to be flat to within 0.5 μm over a 1 cm^2 area. These restrictions require considerable sample preparation for absolute displacement measurements. In contrast, a contact piezoelectric transducer requires the surface

roughness only be considerably less than a wave length in the material. For aluminum at 5 MHz, 10 μm of surface roughness is still less than 0.01 of a wave length. Therefore, the sample preparation required is considerably less, with greater sensitivity. In addition to the general problems of making measurements with capacitive transducers, when the specimen is a non-conducting material (like polymers), the static charge built on the surface makes the measurements of the capacitance ineffective, if not impossible, and invalidates the conversion of measured signals to absolute displacements

It is possible to use a contact transducer for the displacement measurements if a model can be used to convert the output voltage of the transducer to the absolute displacement in the specimen. This requires a physical model which accounts for the electromechanical interaction of the transducer with an applied electric field, as well as the acoustic response of any intermediate layers.

Much work has been done [Berlincourt 1964, Sittig 1969, Leedom 1971, Desilets 1978] to develop models principally for the design of transducer systems with special performance characteristics. Little work has been done to quantitatively compare the results of the models with experimental results, to determine the applicability of these models to

help deconvolve the transducer response to determine the amplitudes of acoustic waves. If accurate, a model could be used in a variety of applications from nonlinear characterization of materials to deconvolving the temperature response of the transducers from thermal derivative measurement. In this chapter we describe a physical model of a transducer bonded to a solid for the absolute displacement measurements of both the fundamental and the harmonic ultrasonic waves. To test the model, some results of the fundamental displacement measurements of some metals are also presented.

4.1 Physical model

To construct such a model, Mason's equivalent circuit [Berlincourt 1964] and Sittig's model for transducers in a layered system [Sittig 1967 and 1969] are used. Following Sittig, the acoustic, dielectric and piezoelectric properties of the transducer, bond, and solid are considered. From these properties, the time domain response of the system is modeled and the input and output voltages are related to the amplitude of the ultrasonic wave.

A typical thickness-mode piezoelectric transducer has lateral dimensions of many wavelengths of sound and negligible attenuation up to hundreds of MHz. Therefore, we consider a plane wave propagating in the lossless transducer

followed by a intermediate layer of bond and then a semi-infinite transmission medium. A separate correction due to attenuation and diffraction in the transmission medium is considered for amplitudes of the received signals.

Fig. 4.1 shows a typical arrangement of a piezoelectric transducer bonded to a transmission medium. Each layer is characterized by a cross-sectional area S and an individual density ρ_n, thickness l_n, and acoustic velocity c_n. In addition, a permittivity ε_n characterizes the dielectric property of a dielectric bond or piezoelectric layer; and an electromechanical coupling factor k_0 is also for the piezoelectric layer. ($n = 0$ for a piezoelectric layer and $n = 1$ for a bond.) By analyzing Mason's equivalent circuits for all layers, the transformation matrix coupling the input voltage E and current i to the force F and particle velocity v of a transducer bonded to a solid can be written as

$$\begin{bmatrix} E \\ i \end{bmatrix} = \begin{bmatrix} A & B \\ C & D \end{bmatrix} \begin{bmatrix} F \\ v \end{bmatrix}, \tag{4.1.1}$$

with

$$\begin{bmatrix} A & B \\ C & D \end{bmatrix} = \frac{1}{\Phi Q} \begin{bmatrix} \eta & j\Phi^2/\omega C_0 \\ j\omega C_0 & 0 \end{bmatrix} \begin{bmatrix} \mathrm{Cos}\gamma_0 & jZ_0\mathrm{Sin}\gamma_0 \\ j\mathrm{Sin}\gamma/Z_0 & 2(\mathrm{Cos}\gamma_0 - 1) \end{bmatrix} \cdot \begin{bmatrix} \mathrm{Cos}\gamma_1 & jZ_1\mathrm{Sin}\gamma_1 \\ j\mathrm{Sin}\gamma_1/Z_1 & \mathrm{Cos}\gamma_1 \end{bmatrix} \tag{4.1.2}$$

where

$$Z_n = \rho_n c_n S \tag{4.1.2a}$$

$$f_n = c_n/2l_n \quad \text{or} \quad \omega_n = \pi c_n/l_n \tag{4.1.2b}$$

$$\gamma_n = \pi f/f_n \tag{4.1.2c}$$

$$C_n = \varepsilon_n S/l_n \tag{4.1.2d}$$

$$\Phi^2 = \omega_0 C_0 Z_0 k_0^2/\pi \tag{4.1.2e}$$

$$Q = \cos\gamma_0 - 1, \tag{4.1.2f}$$

and

$$\begin{aligned} \eta &= 1 && \text{for conducting bonds} \\ \eta &= 1 + C_0/C_1 && \text{for dielectric bonds} \end{aligned} \tag{4.1.2g}$$

Expressions (4.1.2.a)-(4.1.2.g) are represented schematically in the equivalent circuit of Fig. 4.2. Using the transformation matrix, the particle velocity, $v(\omega)$, is related to the source voltage, E_s by

$$v(\omega) = E_s/[AZ_t+B+Z_s(CZ_t+D)], \tag{4.1.3}$$

where Z_s is the source impedance and Z_t ($= \rho c S$) the acoustical impedance of the transmission medium.

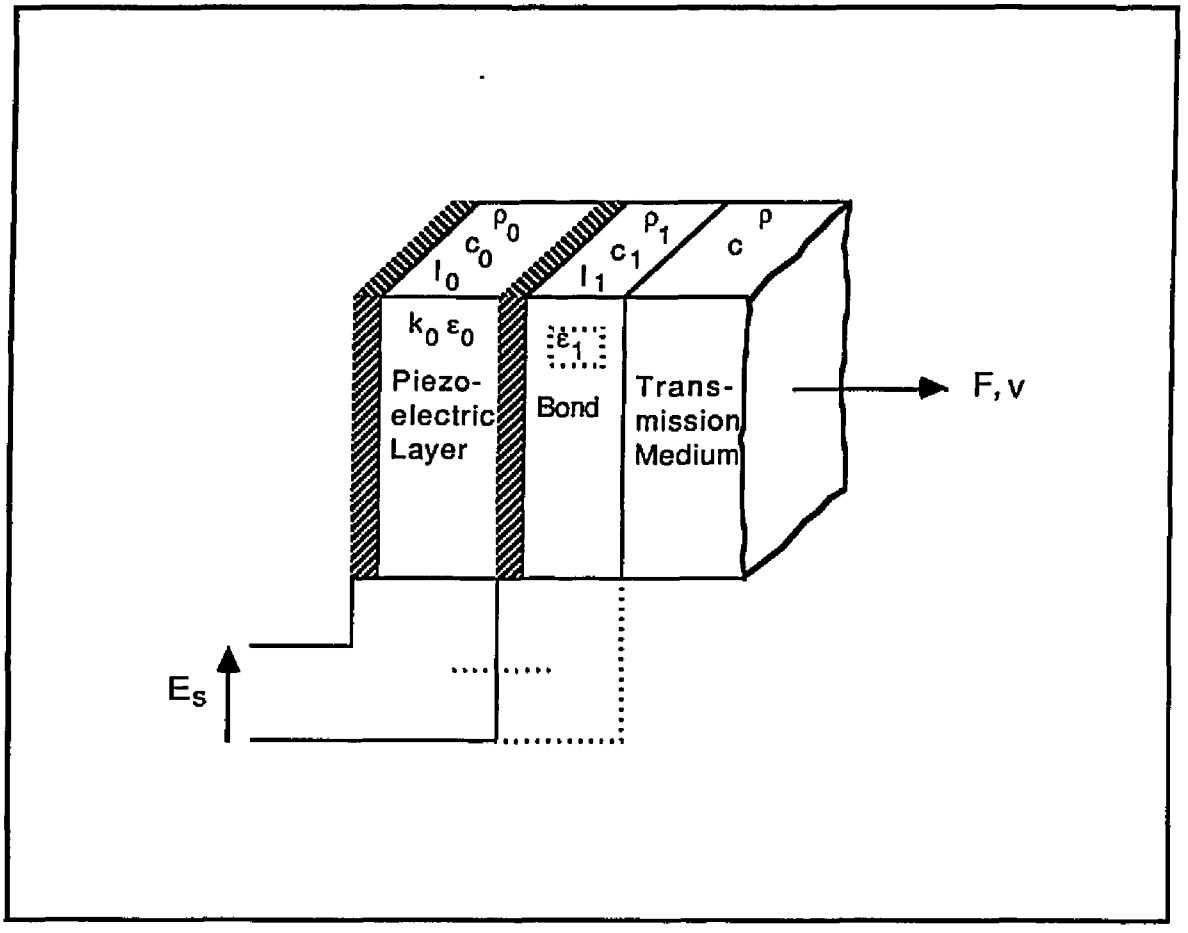

Fig. 4.1 Configuration of a piezoelectric transducer bonded to a solid. The dotted line represents the case for a dielectric bond.

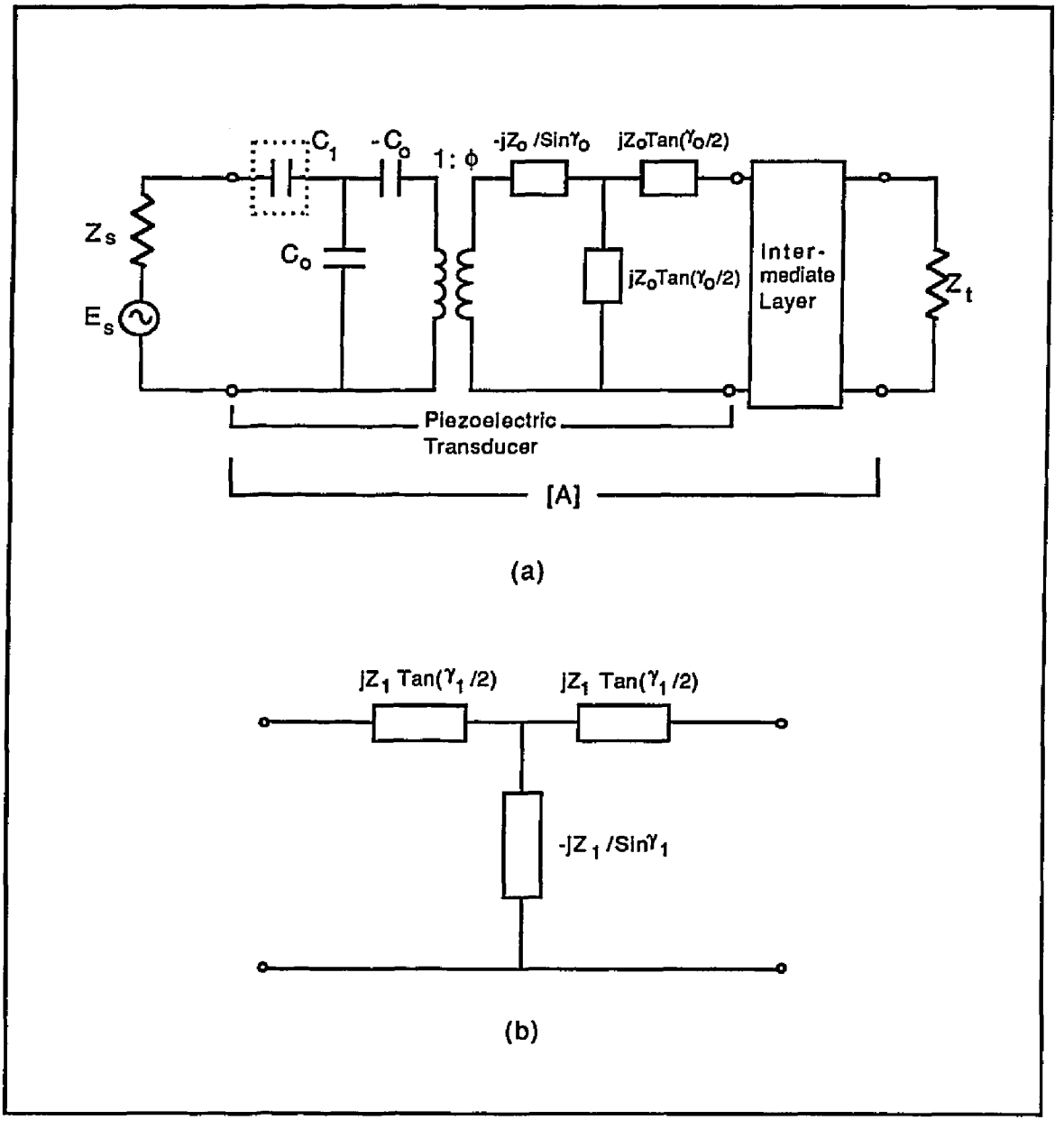

Fig. 4.2 (a) Mason's equivalent circuit for a transducer bonded to a solid of impedance Z_t. [A] represents the Transformation matrix (4.1.2). (b) Equivalent circuit for an intermediate layer (bond).

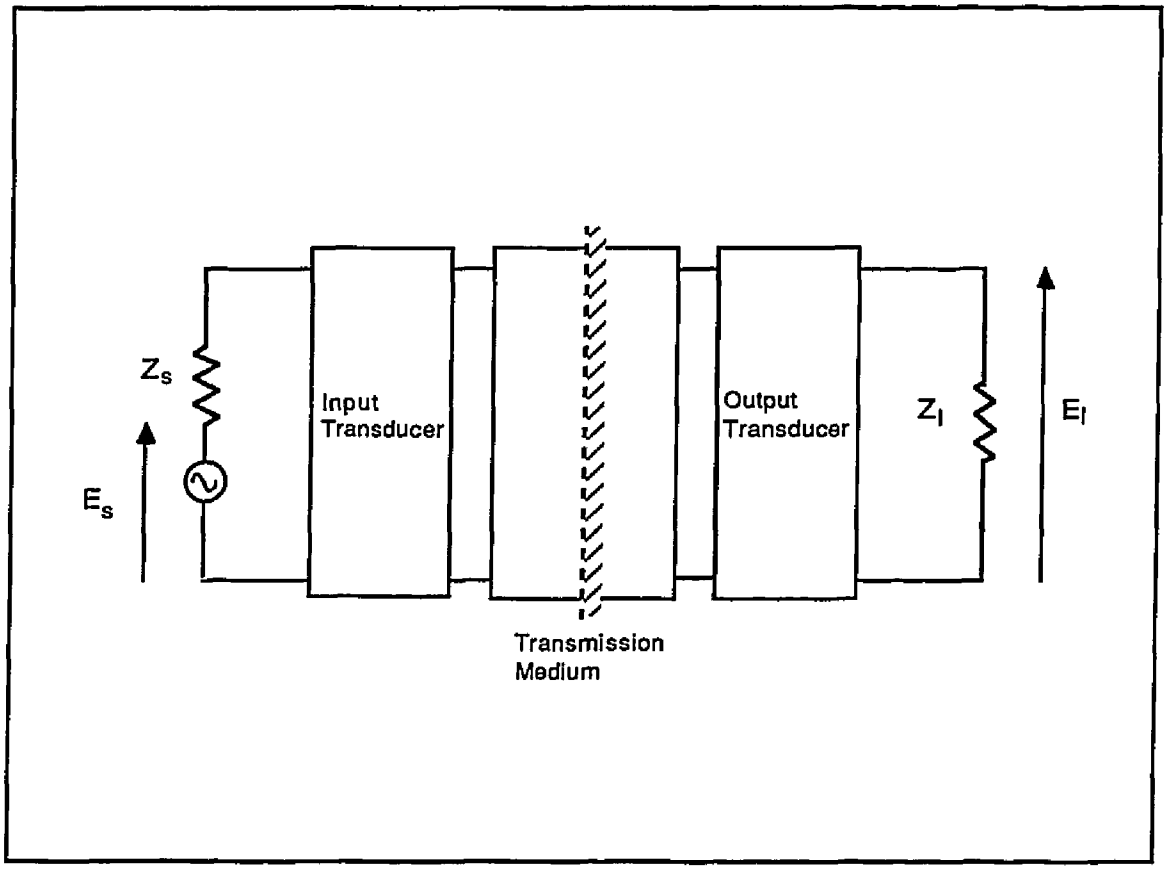

Fig. 4.3 Equivalent circuit for a typical ultrasonic delay line. The shadow on the center represents that the model can be either transmission with two transducers or reflection with one transducer as input and output.

Eq. (4.1.3) gives the relationship between the source voltage and the generated particle velocity in the solid assuming a single frequency excitation. The particle displacement for this type of excitation can be found from the particle velocity using the expression

$$u(\omega) = -jv(\omega)/\omega. \tag{4.1.4}$$

To determine the output voltage of the piezoelectric transducer, the equivalent circuit shown in Fig. 4.3 is used. For an input pulse shorter than the twice the transient time in the transmission medium, there is no interference between the input and output transducers. A pulse-echo response can be modeled by making the receiving transducer identical to the transmitting one, but operated in reverse. Therefore, the transformation matrix for the receiving transducer can be obtained by exchanging A and D of (4.1.1). The resulting voltage transfer ratio between the source and the load is given by

$$\frac{E_1}{E_s} = \frac{2Z_tR_1}{[AZ_t+B+Z_s(CZ_t+D)][AZ_t+B+Z_1(CZ_t+D)]}, \tag{4.1.5}$$

where R_1 is the resistive part of the load impedance, Z_1. Eq. (4.1.5) gives the relationship at a single frequency. To obtain theoretically the impulse response, the Fourier

transform of Eq. (4.1.5) is taken. For a response to an arbitrary input signal, the input is convolved with the impulse response to calculate the time dependence of the output of the transducer. A similar process can be used to obtain the time dependence of the displacement u(t).

In (4.1.3), $v(\omega)$ is expressed in terms of the source voltage. By substituting (4.1.5) into (4.1.3) and using (4.1.4), the relation between the displacement and the output voltage of the receiving transducer is obtained as

$$u(\omega) = -jE_1 \frac{[AZ_t+B+Z_1(CZ_t+D)]}{2\omega Z_t R_1} . \qquad (4.1.6)$$

By evaluating the transformation matrix elements and the impedances, in other words, making a calibration for the measuring system, the amplitude of the fundamental and the second harmonic, and hence the nonlinearity parameter β_3 can be calculated.

4.2 Model Results

To test the model, a lithium niobate—36° Y-cut crystal was chosen as the longitudinal transducer. lithium niobate transducers are widely used in ultrasonic devices because of

their large electromechanical coupling constant and high Curie temperature (~1200° C). The elastic, piezoelectric, and dielectric constants of Lithium Niobate and their temperature dependence have been measured by several authors [Warner 1967, Smith 1971]. For our calculation, the values are taken from Smith et al [Smith 1971]. Using these values, the capacitance of the transducers were calculated and found to be within 0.5% of the measured values. The capacitance of the bond was determined by measuring the total capacitance of the bond and the transducer in series. Also the acoustic impedances (the density and the sound velocity) of the bond and the specimen were measured. All the results were used to determine the transformation elements and the impedances for the model.

The model was used to calculate the response of a lithium niobate transducer bonded to several different materials. A typical response of the output transducer is shown in Fig. 4.4, where a lithium niobate transducer is modeled to be bonded to aluminum with phenyl salicylate. For thin bonds, the thickness of the bond has a greater effect on the response decay than on its amplitude. A measured response is shown with the modeled response in Fig. 4.4. The modeled response has been corrected for diffraction losses using Khimumin's tables [Khimunin 1972]. As can be seen from Fig. 4.4, the agreement between the model and the measure-

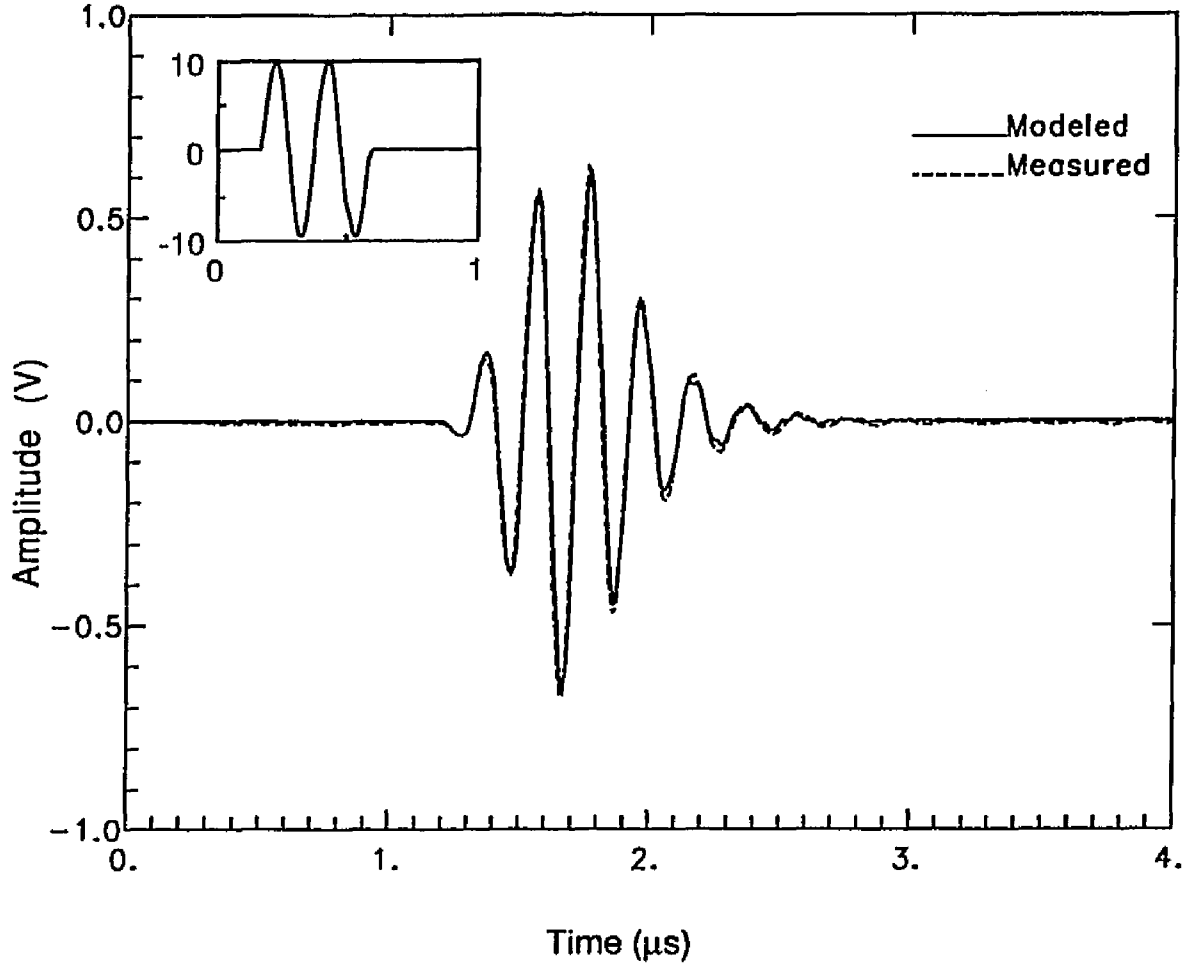

Fig. 4.4 Comparison of the measured and the modeled response of a lithium niobate transducer bonded to A16061 with phenyl salicylate. The effective bond thickness about 6 μm is taken for the model. The input signal, shown in the upper-left corner, is a 5MHz-2cycle sine wave.

ment is excellent. Such agreement suggests that the transformation matrix should be well-defined and it be possible to calculated the absolute displacements directly from either the input drive or the output received signal. The next section discusses a comparison of this calculation to an independent measurement with a capacitive transducer.

4.3 Accuracy of Absolute Displacement Measurements with Contact Transducers

To determine the accuracy of the technique, measurements with a capacitive detector were made on aluminum, brass and steel samples. For each drive voltage applied to the lithium niobate, the sample was rotated five times and a measurement taken at each orientation. The measurements for different rotations were averaged and the standard deviation found to be 2%, which is typical for the capacitive detector. The amplitude of the ultrasonic wave generated in aluminum for different drive voltages is shown in Fig. 4.5. Also plotted in Fig. 4.5 is the amplitude of the ultrasonic wave calculated from the model as a function of drive voltage. The figure indicates the excellent agreement between the data and the model. The ratios of amplitude to drive voltage as found from the experiment and model for several different samples are given in Table 4.1. The measurements in brass

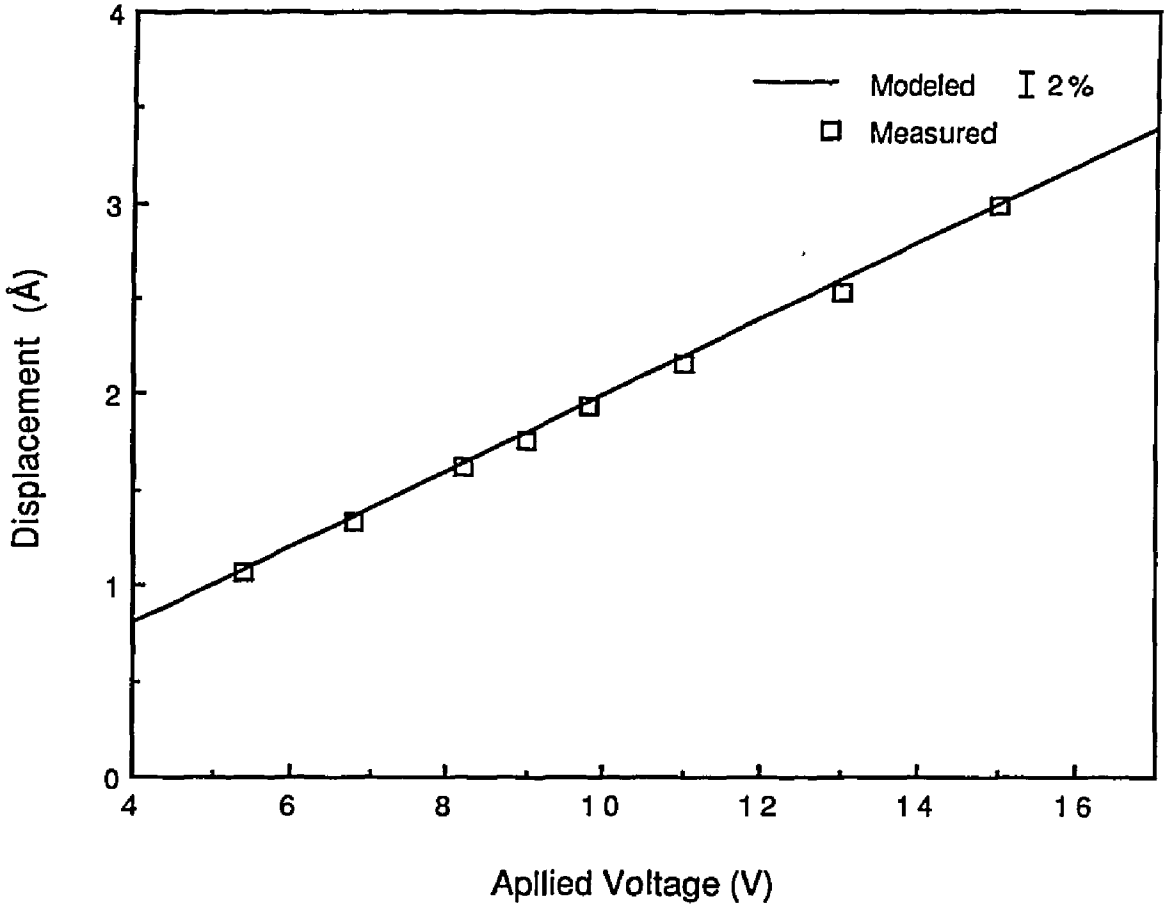

Fig. 4.5 Comparison of the calculated displacements in Al 6061 from the model and measured from the capacitive detector. The error bar represents the error of ±2% for the modeled displacements.

TABLE 4.1

Comparison of the Modeled and the Measured Displacements for Various Samples

Sample	Displacement/Drive-voltage (Å/V)	
	Modeled	Capacitive Detector
Al 6061	0.199 ± 0.004	0.198 ± 0.005
Brass	0.091 ± 0.003	0.092 ± 0.003
Steel	0.084 ± 0.003	0.085 ± 0.003

and steel were corrected for attenuation, as well as diffraction. As can be seen from the table the excellent agreement between the model and the measurements is true for materials with a wide range of acoustic properties.

The model presented in this chapter predicts quantitatively the response of piezoelectric transducers, which is very useful for deconvolution of the transducer response in ultrasonic measurements.

We have also shown that the model predicts the absolute amplitudes of ultrasonic waves generated in solids to within 2% of that measured by a capacitive detector. Therefore, with this model, it is possible to measure the absolute amplitudes of ultrasonic waves in solids with Lithium Niobate transducers. The model therefore offers an attractive alternative to the capacitive transducer for these measurements.

In the next two chapters we conduct an investigation using this model to determine the nonlinear properties of polymers, for which the displacement measurements of the fundamental and second harmonic waves are required.

V. EXPERIMENT AND ANALYSIS

5.1 The Measurements of β_3

As shown in Chapter IV, the measurement of the nonlinearity parameter β_3 can be accomplished using contact piezoelectric transducers. In this section we describe the details of using lithium niobate transducers to measure the fundamental and second harmonic displacements for polymers.

The experimental apparatus used to measure the fundamental and second harmonic is shown in the block diagram of Fig. 5.1. A function generator was used to generate the gated rf bursts Any spurious high frequency content of the amplified rf burst is reduced through filtering with an analog low pass filter before being used to drive the transducer. A 5MHz lithium niobate longitudinal transducer was bonded to one side of the specimen, as a transmitter, and a 10MHz transducer to the other side, as a receiver of both the fundamental and the harmonic waves. For the measurement of the harmonic, the output of the 10MHz transducer was filtered through an analog high pass filter before being

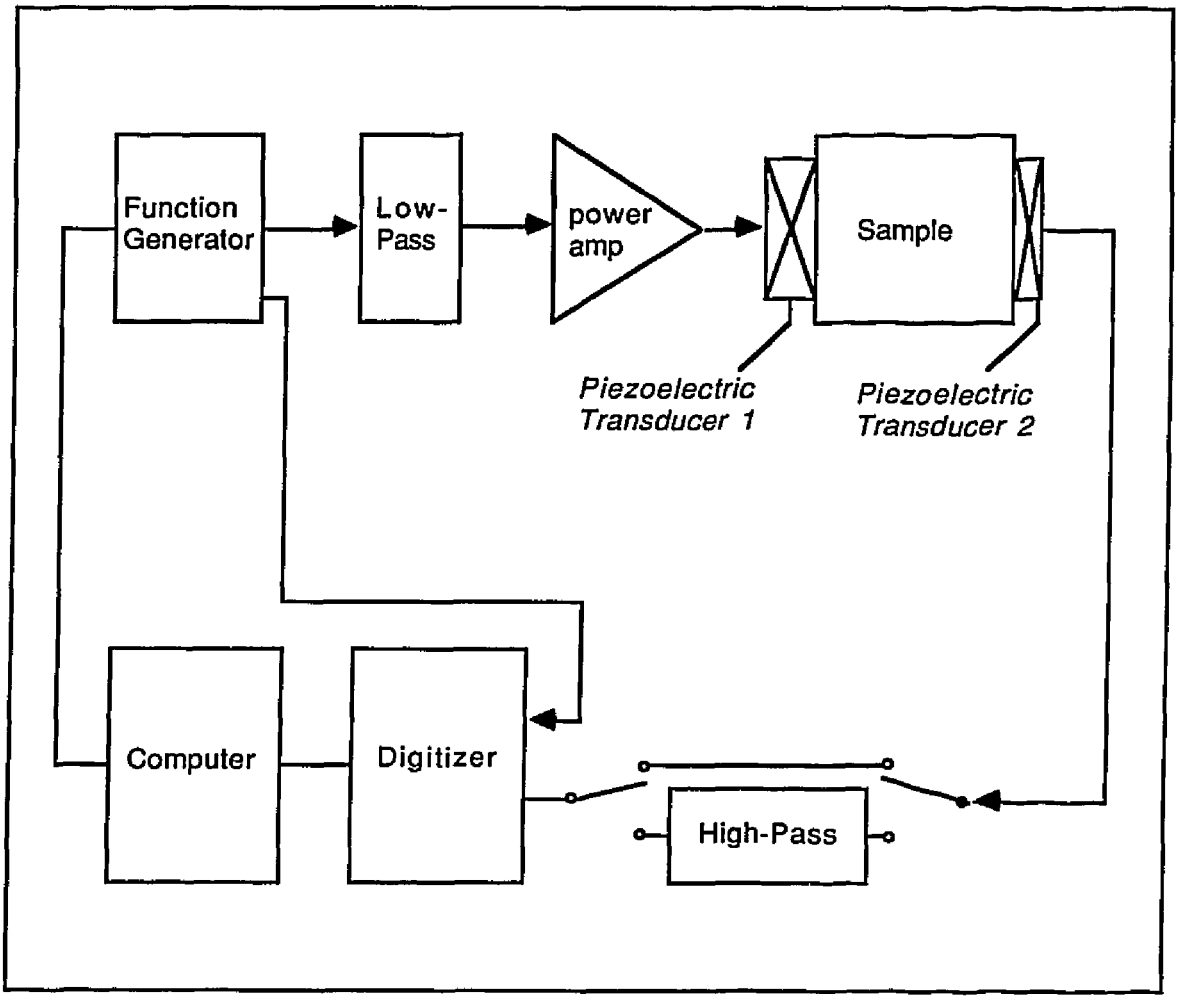

Fig. 5.1 Block diagram of the measurement system with piezoelectric transducers for harmonic generation.

digitized, then transferred to the minicomputer for off-line processing and storage. For the fundamental, signals were digitized without the filter. The measurement was repeated with several different drive amplitudes for each specimen.

After finishing each set of measurements, the load impedance of the receiver (Z_1 as described in section 4.1) was determined for frequencies over the range of interest by using a impedance analyzer. Each set of impedances was recorded for use in later analysis.

The fundamental and second harmonic displacements are required for calculating the nonlinearity parameter β_3. The measured signal is a convolution of the ultrasonic wave with the impulse response of the detection system. The impulse response can be calculated by calibrating the transducer (evaluating the transformation matrix elements), measuring the load impedance, and using the formalism as described in section 4.1. By deconvolving the impulse response of the system from the measured electric signal, the absolute displacement of the ultrasonic wave can be calculated. For illustrating this process, it is convenient to rewrite (4.1.6) as

$$u(\omega) = E_1(\omega)/L(\omega), \qquad (5.1.1)$$

where

$$L(\omega) = 2j\omega Z_t E_1 / [AZ_t+B+Z_1(CZ_t+D)] \qquad (5.1.2)$$

the Fourier transform of the impulse response of the receiver, with all the quantities defined in section 4.1. The Fourier transform $E_1(\omega)$ of the measured signal is deconvolved and the Fourier transform $u(\omega)$ of the absolute amplitude of the ultrasonic wave is then obtained. Since the right hand side of the Eq.(5.1.1) has a pole for the frequency equal to zero, the Fourier transform is evaluated only over the frequency range of interest. The inverse transform of this result, u(t) is a time record of the ultrasonic displacement in the specimen.

In Fig. 5.2 a typical recorded signal, $E_1(t)$, from polysulfone is displayed. The fundamental and the second harmonic signals are superimposed in the output of the transducer; the asymmetry about zero of the signal indicates the contribution from the harmonic is appreciable. The Fourier transform of the signal, $E_1(\omega)$, is shown in Fig. 5.3. The larger amplitude signal indicates the main frequency of the fundamental; the signal at twice the frequency is its second harmonic. After the signal is deconvolved, the inverse Fourier transforms of the fundamental and the harmonic are taken, which are shown in Figs. 5.4 and 5.5 respectively.

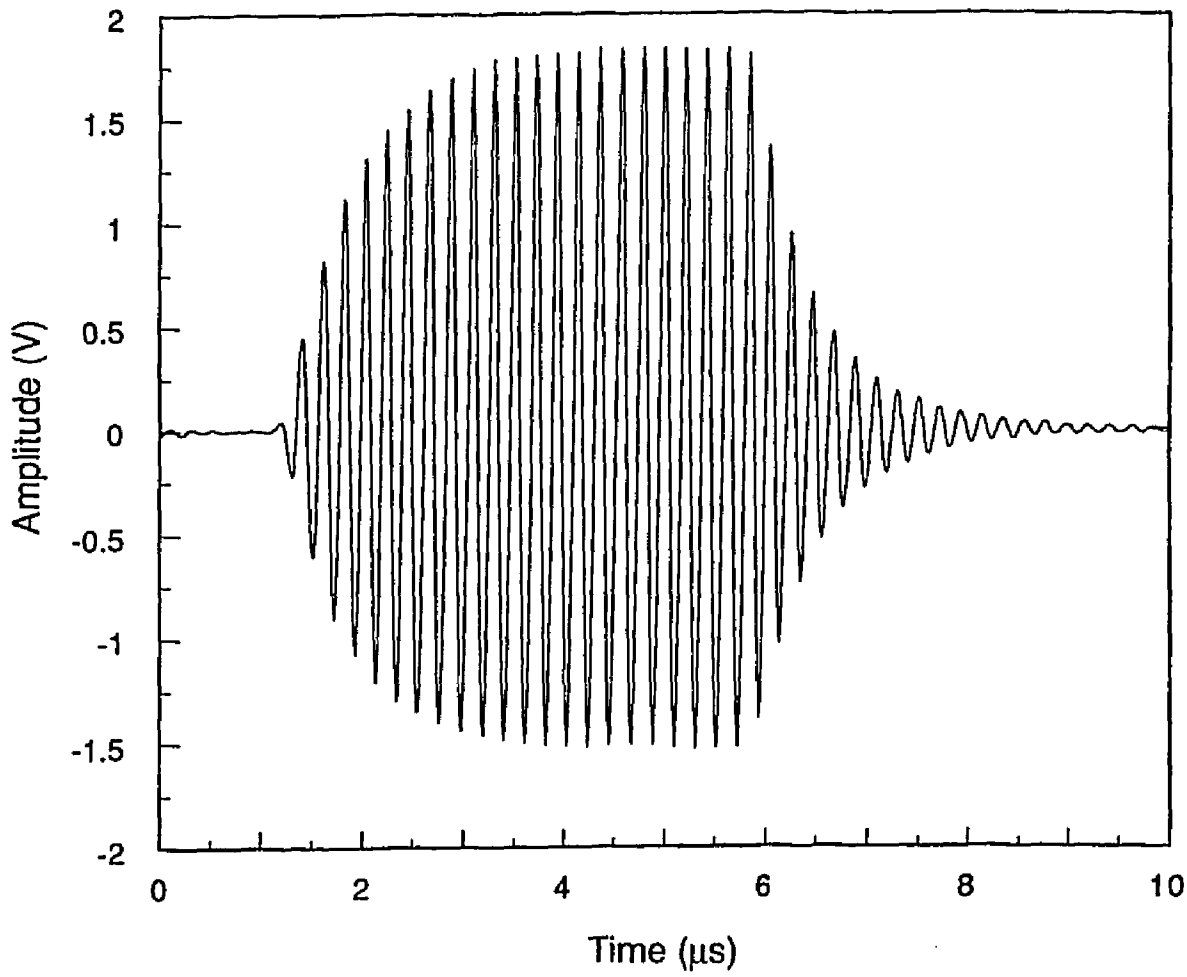

Fig. 5.2 The typical recorded signal from the output of the transducer for the harmonic generation of polysulfone. The fundamental and the second harmonic signals are superimposed.

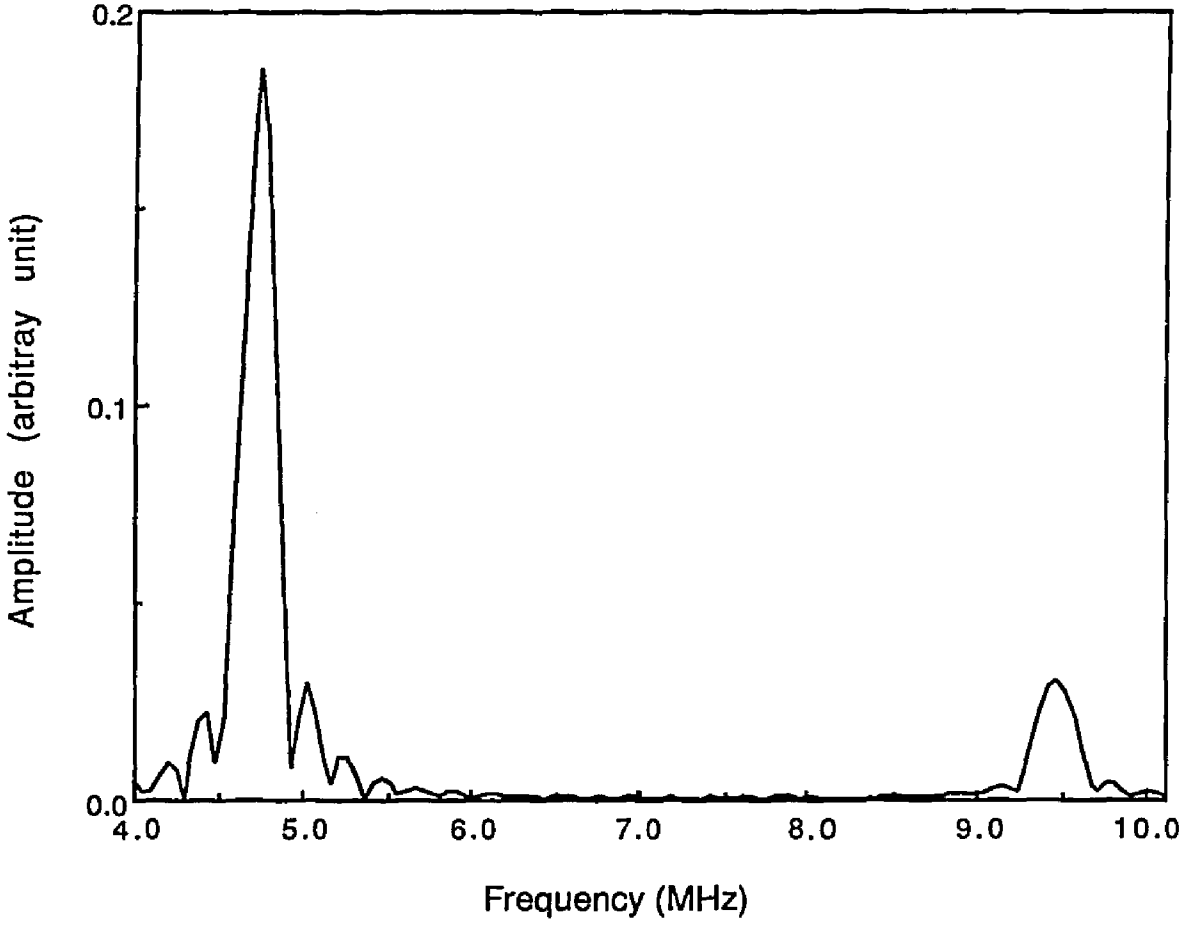

Fig. 5.3. The Fourier transform of the signal shown in Fig. 5.2.

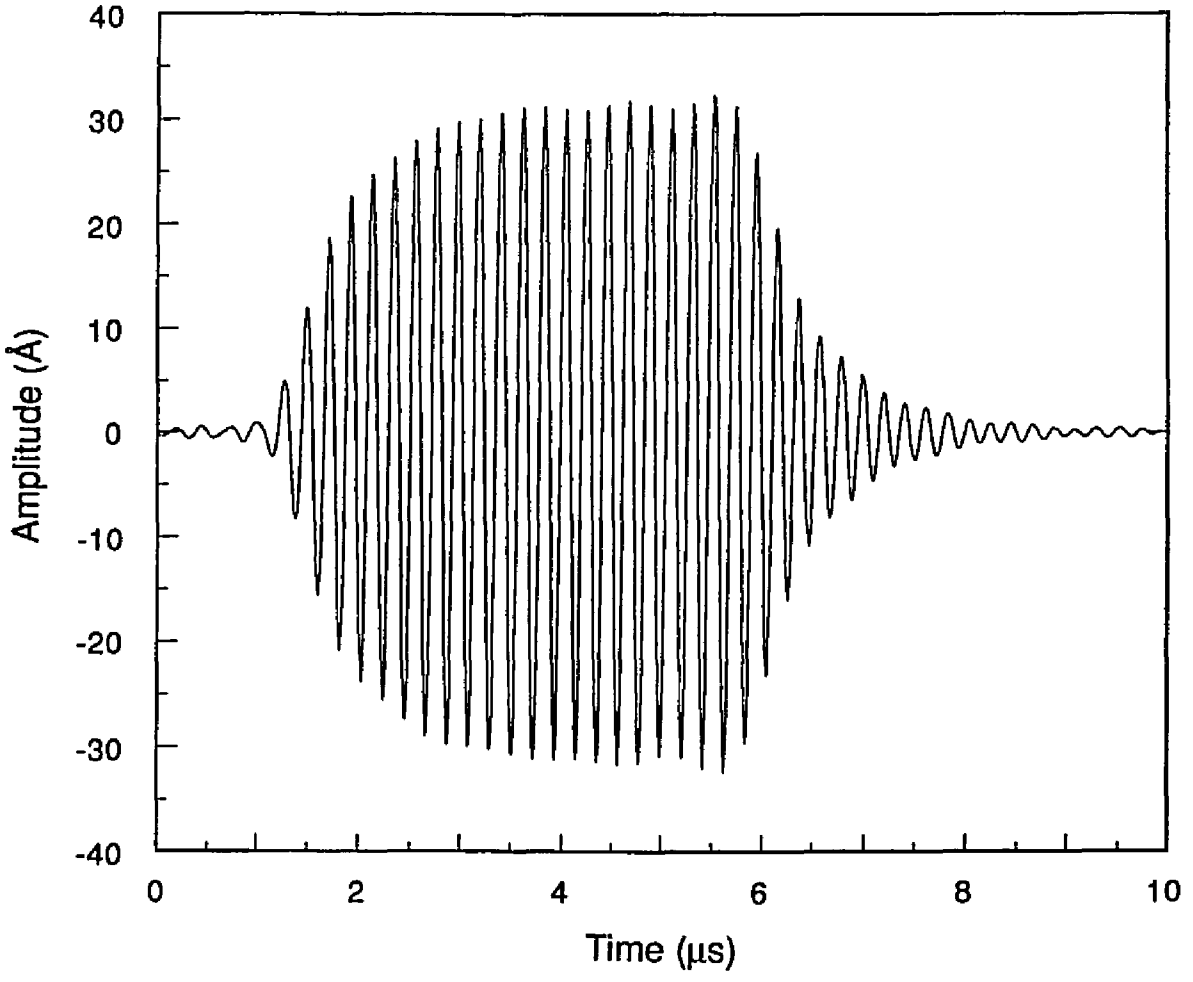

Fig. 5.4 The fundamental displacement deconvolved from the recorded signal.

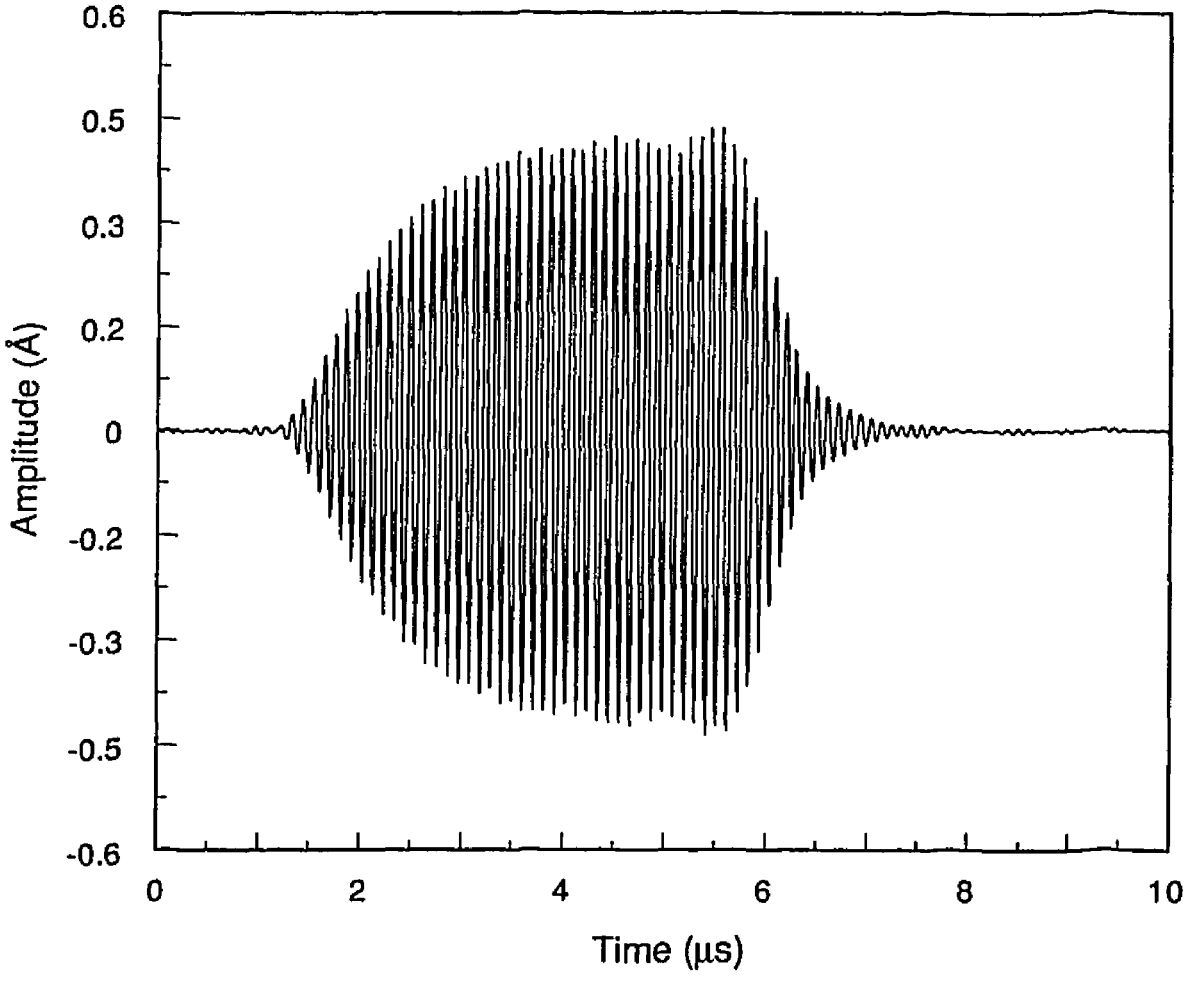

Fig. 5.5 The second harmonic displacement deconvolved from the recorded signal.

(The digitized signals are recorded as a time step of 10ns per point. The Fourier transform of the signal is a result of a numerical 2048-point-Fast-Fourier-Transformation. The frequency resolution is about 0.05MHz per point. The result shown in Fig. 5.3 is the FFT of the signal in Fig. 5.2 for the width of 10μs.)

5.2 The Attenuation Correction for the Harmonic Generation

In section 2.1 the medium is assumed to be nondissipative, in which the fundamental wave travels and the second harmonic is generated. In a practical situation the material is somewhat dissipative and the attenuation is frequency dependent as well; therefore, a correct calculation of the nonlinearity parameter requires a correction for the effects of attenuation.

We limit our consideration to materials where the attenuation is small enough so that the plane wave solutions are not critically damped. This condition can be expressed as $\alpha\lambda \ll 1$, where α is the attenuation coefficient and λ the wavelength, which is true at ultrasonic frequencies even for relatively highly attenuating polymers. For example, at room temperature, the value of $\alpha\lambda$ is only about 0.046 for PSF

with a attenuation coefficient of about 1Np/cm (8.686db/cm) at 5MHz, the highest attenuation of the three investigated polymers. We also assume the fundamental and the generated harmonic are independently attenuated.

The amplitude of an attenuated fundamental wave can be expressed as

$$A_1 = A_0 \exp(-\alpha_1 l), \tag{5.2.1}$$

where α_1 is the attenuation coefficient of the fundamental wave and A_0 the wave amplitude at $l = 0$. At any point, l, the second harmonic is being generated by the fundamental as well as being dissipated by loss mechanisms. As a result the amplitude is given by

$$dA_2/dl = wA_1^2 - \alpha_2 A_2, \tag{5.2.2}$$

where $w = |\beta_3| k^2/8$, a constant proportional to the nonlinearity parameter and α_2 is the attenuation coefficient of the second harmonic. The solution of (5.2.2) can be expressed as

$$A_2(l) = wA_0^2 \, e^{-\alpha_2 l} \left(\frac{1 - e^{-(2\alpha_1 - \alpha_2)l}}{2\alpha_1 - \alpha_2} \right) . \tag{5.2.3}$$

For a nondissipative solid the ratio of A_2 to A_1^2 is given by the expression

$$|A_2/A_1^2| = wl \tag{5.2.4}$$

for a dissipative solid, according to (5.2.3) the ratio becomes

$$\begin{aligned} |A_2/A_1^2| &= wl\exp(\delta l)[1 - \exp(-\delta l)]/(\delta l) \\ &= wl[\exp(\delta l) - 1]/(\delta l), \end{aligned} \tag{5.2.5}$$

where $\delta = 2\alpha_1 - \alpha_2$. Therefore, the attenuation correction factor required for determining the nonlinearity parameter, in a dissipative solid, is $\delta l/[\exp(\delta l) - 1]$. It is interesting to note that for an attenuation coefficient linearly proportional to frequency, f ($2\alpha_1 = \alpha_2$), expression (5.2.5) becomes $|A_2/A_1^2| = wl$ with $\delta = 0$, which has the same form as for a nondissipative solid.

The ultrasonic attenuation of polymers typically has a linear dependence on frequency [Hartman 1972], expressed as

$$\alpha = a + bf \tag{5.2.6}$$

where a and b are constants, and f is the frequency, over the frequency range from 10^0 to 10^7 Hz at room temperature.

For this functional dependence of attenuation δ, the size of the attenuation correction is given by

$$\delta = a. \tag{5.2.7}$$

Near room temperature and in the frequency range of low MHz, the attenuation of all the investigated polymers is dominated by the linearly-frequency-dependent component; therefore δ is small. For PMMA δ is about 0.5 db/cm or 0.058/cm at room temperature [Hartmann 1972, Asay 1969], which results in an approximately 3% per cm correction. For PS and PSF the value is even smaller. [Phillips 1977] Hence, the nonlinearity parameter, to a good approximation, can be evaluated directly from the attenuated amplitudes of the fundamental and the second harmonic for these polymers.

5.3 The Measurement of Temperature and Pressure Dependence of Ultrasonic Velocity

As described in Sec. 2.2, the nonlinearity parameter can also be calculated from the pressure and temperature coefficients of acoustic velocity with various thermal constants. For comparison with the results from harmonic generation, the acoustic data required was obtained from the literature when available, or from measurements. While only

the longitudinal velocities are necessary for calculating acoustic nonlinearity parameters, we also measured the shear velocities as functions of temperature and/or pressure for calculating the Grüneisen parameters as described in section 2.3.

For measuring temperature dependence of the velocity, the specimen was put in the temperature controller, described in section 3.2. About 100 min was allowed for each setting of temperature to ensure that the specimen had reached thermal equilibrium to within ±0.02°C before measurements were taken. The initial transit time at room temperature and atmospheric pressure was measured first; and then the transit time measurements were taken over the temperature range of 22°-40°C.

A pitch-catch method was used to measure the change of velocity with temperature. Each side of the specimen was bonded to an identical 5MHz lithium niobate transducer (36° Y-cut for the longitudinal and 41° X-cut for the shear).

For measuring the pressure dependence of velocities, the pressure system shown in section 3.2 was used. To reduce the number of leads and keep the structure of the chamber simple, a pulse-echo method was used to measure the velocity change with pressure. The temperature was isothermally controlled at 25°C. After each setting of pressure a period

of about 100 min was allowed for thermal equilibrium of the system and the specimen. Measurements were made over the pressure range of 0-1.7 MPa (0-250 psi).

Since, in ultrasonic measurements the parameter measured directly is the transit time, it is convenient to define a pressure coefficient of the transit time,

$$\kappa_l(T_0) \equiv -\frac{1}{\tau_{l,0}}\left(\frac{\partial\tau_l}{\partial p}\right)_{T,p=p_0} = -\left(\frac{\partial \ln\tau_l}{\partial p}\right)_{T,p=p_0} , \qquad (5.3.1)$$

where $\tau_{l,0}$ is transit time at $p = p_0$ for the longitudinal wave. Similarly for the shear wave,

$$\kappa_t(T_0) \equiv -\frac{1}{\tau_{t,0}}\left(\frac{\partial\tau_t}{\partial p}\right)_{T,p=p_0} = -\left(\frac{\partial \ln\tau_t}{\partial p}\right)_{T,p=p_0} . \qquad (5.3.2)$$

Also for the temperature dependence of ultrasonic velocity, the temperature coefficients of the transit time are defined as,

$$\eta_l(T_0) \equiv \left(\frac{\partial \ln \tau_l}{\partial T}\right)_{p,T=T_0}, \tag{5.3.3}$$

and

$$\eta_t(T_0) \equiv \left(\frac{\partial \ln \tau_t}{\partial T}\right)_{p,T=T_0}. \tag{5.3.4}$$

From the relationship of the ultrasonic velocity and the transit time, the expression

$$\ln c = \ln l - \ln \tau. \tag{5.3.5}$$

can be obtained. Hence, the pressure coefficient of the longitudinal velocity can be related to the pressure coefficient of the transit time as

$$\left(\frac{\partial \ln c_l}{\partial p}\right)_T = -\left(\frac{\partial \ln \tau_l}{\partial p}\right)_T + \left(\frac{\partial \ln l}{\partial p}\right)_T = \kappa_l - \frac{1}{3}\beta_T, \tag{5.3.6}$$

where $(\partial \ln l/\partial p)_T = 1/3\ (\partial \ln V/\partial p)_T = -\beta_T/3$. Similarly, the temperature coefficient of the longitudinal velocity,

$$\left(\frac{\partial \ln c_l}{\partial T}\right)_p = -\eta_l + \frac{1}{3}\alpha \quad . \tag{5.3.7}$$

By substituting (5.3.6) and (5.3.7) into (2.2.23) and (2.2.24) respectively, the constants K_T and K_p, which are are related to the nonlinearity parameter B/A, become

$$K_T = \frac{1}{\beta_T}\left(\frac{\partial \ln c_l}{\partial p}\right)_T = \frac{\kappa_l}{\beta_T} - \frac{1}{3} \tag{5.3.8}$$

and

$$K_p = -\frac{1}{\alpha}\left(\frac{\partial \ln c_l}{\partial T}\right)_p = \frac{\eta_l}{\alpha} - \frac{1}{3} \quad . \tag{5.3.9}$$

According to these expressions we can calculate K_T and K_p, and thereafter nonlinearity parameter B/A, from the measured coefficients κ_l and η_l.

To calculate the Grüneisen parameter, both the longitudinal and shear transit time coefficients are needed. According to Eq.(2.3.6b)

$$\Gamma_T = \frac{1}{\beta_T}\left(\frac{\partial \ln c_s}{\partial p}\right)_T + \frac{1}{3} \quad ,$$

the pressure coefficient of the the average sound velocity is required. Since

$$c_s = \left[\frac{1}{3}\left(c_l^{-3} + 2c_t^{-3}\right)\right]^{-1/3} = l\left[\frac{1}{3}\left(\tau_l^3 + 2\tau_t^3\right)\right]^{-1/3},$$

one obtains

$$\left(\frac{\partial \ln c_s}{\partial p}\right)_T = \frac{-\left(\tau_l^2 \frac{\partial \tau_l}{\partial p} + 2\tau_t^2 \frac{\partial \tau_t}{\partial p}\right)}{\tau_l^3 + 2\tau_t^3} + \frac{\partial \ln l}{\partial p}$$

$$= \frac{\tau_l^3 \kappa_l + 2\tau_t^3 \kappa_t}{\tau_l^3 + 2\tau_t^3} - \frac{1}{3}\beta_T \quad . \qquad (5.3.10)$$

It is convenient to define an average pressure coefficient of the transit time:

$$\kappa_s \equiv \frac{\tau_l^3 \kappa_l + 2\tau_t^3 \kappa_t}{\tau_l^3 + 2\tau_t^3} = \frac{\kappa_l + 2\zeta^3 \kappa_t}{1 + 2\zeta^3}, \qquad (5.3.11)$$

where

$$\zeta \equiv \tau_t/\tau_l = c_l/c_t; \qquad (5.3.12)$$

such that Eq.(5.3.10) becomes $-(\partial \ln c/\partial \ln V)_T = \kappa_s/\beta_T - 1/3$, similar to Eq. (5.3.8) with κ_s replacing κ_l.

The Grüneisen parameter is then given by

$$\Gamma_T = \kappa_S/\beta_T, \tag{5.3.13}$$

that is, the Grüneisen parameter can be calculated from the average pressure coefficient of the transit time and the isothermal compressibility. It is interesting to note that the expression (5.3.13) retains the simplicity of the original definition of the Grüneisen parameter, as expression (2.3.4) (the relative change of Debye frequency ω_D corresponding to the pressure coefficient of the transit time, κ_S: and the relative change of the volume corresponding to the compressibility β_T).

VI. RESULTS AND DISCUSSION

6.1 The Calculation of β_3

The nonlinearity parameter is calculated from the amplitudes of the fundamental and second harmonic waves by using Eq. (2.1.5). The measured shape of the fundamental is used for f(t), giving the theoretical wave form of the second harmonic h(t) as

$$h(t) = (1\beta_3/4c^2)[\partial f(t)/\partial t]^2, \qquad (6.1.1)$$

with the parameter β_3 undetermined. The time derivative of the fundamental is calculated by taking the Fourier transform of the signal, multiplying by the frequency and applying the inverse transform. This process eliminates the low frequency parts. However it does not affect the magnitude of the Fourier transform of h(t) in the frequency range of interest.

To determine the nonlinearity parameter, one can simply fit the Fourier transform of the measured second harmonic

waveform by the Fourier transform of h(t) (in the frequency domain instead of the time domain) with the nonlinearity parameter as the only independent variable.

As described in section 5.2, there is a correction for attenuation which is given by Eq. (5.2.5). Therefore, when the measured (attenuated) fundamental wave form is used to generate the theoretical second harmonic, the corrected value for the nonlinearity parameter is given by

$$|\beta_3| = \{\delta l/[\exp(\delta l) - 1]\}|\beta_3'|, \qquad (6.1.2)$$

where $|\beta_3'|$ is the magnitude of the nonlinearity parameter calculated directly from the measured waveforms.

For PMMA δ is 0.0288/cm; δl is much less than 1 for samples of interest. Therefore, the correction factor is reduced to $1 - \delta l/2$. The resulting β_3 for PMMA from three samples with different thickness are shown in Table 6.1. For PS and PSF, δ is nearly zero so the correction factor is 1.

After correcting for attenuation, the corrections for diffraction are considered as well. For the fundamental, the correction factor C_1 is from Khimunin's tables, as mentioned in section 3.2. For the second harmonic the diffraction is much more complicated; nevertheless, the case is similar to

that of attenuation: the second harmonic is generated by the fundamental wave traveling through the medium and is diffracted as it continues to propagate. Neglecting its own diffraction, the second harmonic has an identical transverse spatial dependence as the fundamental wave. Therefore, C_1 is taken as the correction factor for both the fundamental and the second harmonic. The uncorrected β_3 needs to be multiplied by a factor of C_1. All the reported β_3's have been corrected in this way. Table 6.1 gives values of directly calculated β_3 for PMMA, then the values after the attenuation and diffraction corrections, to indicate the relative size of these corrections.

The nonlinearity parameters from the averaged results of all samples measured for three polymers are shown in Table 6.2. Also reported in Fig. 6.1 is the nonlinearity parameter as a function of temperature in the range of 25°-36°C for polysulfone. As can be seen from that figure, the temperature dependence of the nonlinearity parameter is relatively weak, which is typical for most solids well above their Debye temperatures

TABLE 6.1

The Correction of Attenuation and Diffraction for β_3 of PMMA

Sample	1	2	3
Thickness (cm)	1.877	1.325	1.095
Uncorrected	-15.2 ± 0.3	-14.9 ± 0.2	-14.8 ± 0.3
Corrected for attenuation*	-14.8 ± 0.6	-14.7 ± 0.5	-14.6 ± 0.6
Corrected for diffraction‡	-13.2 ± 0.7	-13.4 ± 0.6	-13.3 ± 0.7
Average		-13.3 ± 0.7	

*The values in this row are obtained from those above multiplied by $(1 + \delta 1/2)$.

‡The values in this row are obtained from those above multiplied by C_1.

TABLE 6.2

The Nonlinearity Parameter β_3 for Three Polymers at 25°C and Atmospheric Pressure

Polymer	β_3
Polymethyl methacrylate (PMMA)	-13.3 ± 0.7
Polystyrene (PS)	-11.1 ± 0.8
Polysulfone (PSF)	-10.9 ± 0.6

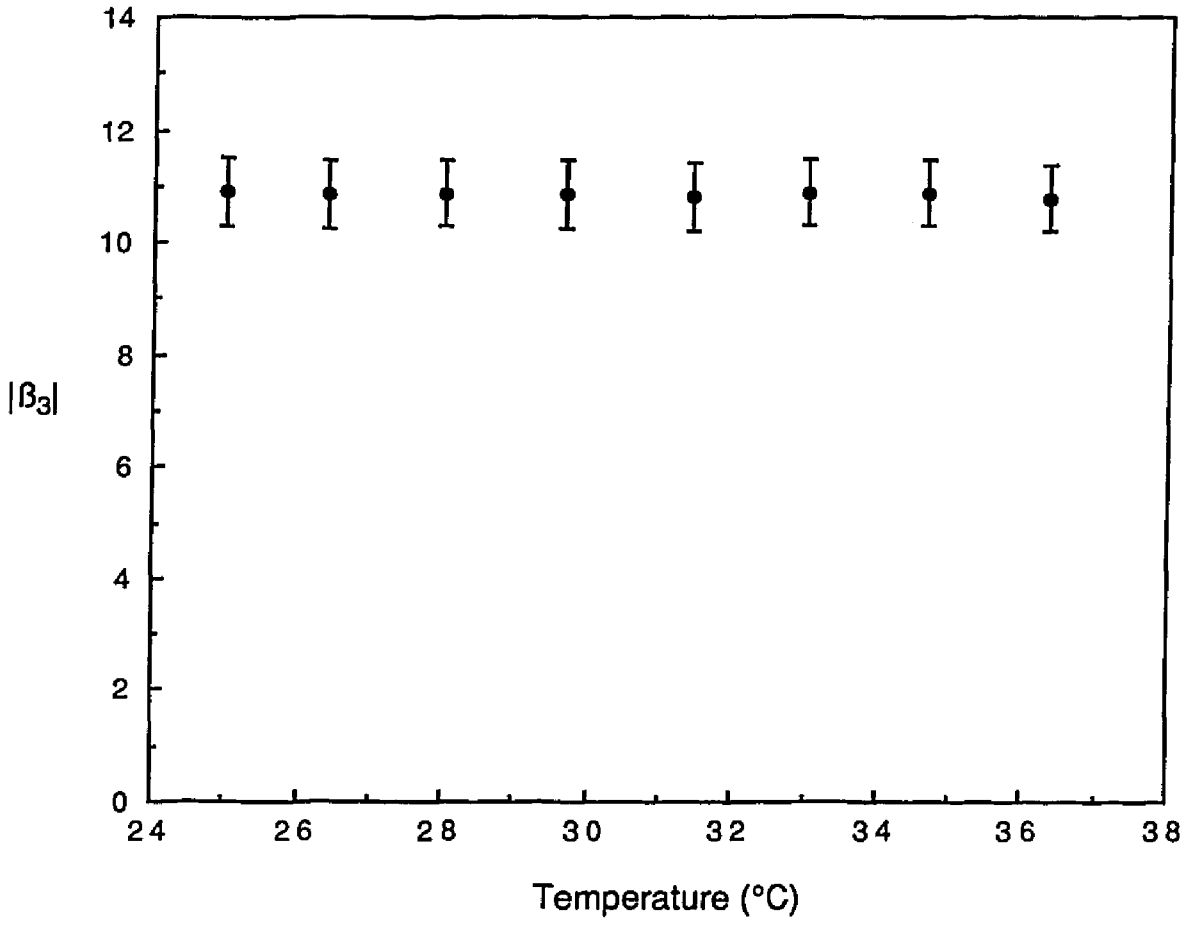

Fig. 6.1 The nonlinearity parameter β_3 as a function of temperature for polysulfone.

6.2 The Temperature and Pressure Coefficients of Ultrasonic Velocities

The ultrasonic velocities for three polymers were first measured at room temperature and atmospheric pressure. The results of both longitudinal and shear velocities at 5 MHz are shown in Table 6.3. Compared with the results in the literature for PMMA and polystyrene [Asay 1969, Lamberson 1972], the agreement is within 0.2%. Also listed in Table 6.3 are the velocity ratio ζ and Poisson's ratio σ. Among the three polymers, polysulfone has the largest values of both ratios.

To determine the temperature coefficient of the transit time for polysulfone at room temperature, the relative change of the transit time is obtained by determining the time shift necessary to curve-fit each recorded waveform with the reference one. The results for longitudinal and shear waves in polysulfone are shown in Fig. 6.2 and 6.3 respectively. Data in those figures represent the relative change of the transit time $(\tau/\tau_0 - 1)$ as a function of temperature. The slopes calculated from linear least-square-fits of these data are the temperature coefficients of the relative transit time, η_l and η_t at 25°C. The temperature coefficients of the velocity are then calculated from temperature coefficients of the transit time using literature

values of the thermal expansion coefficient in Eq. (5.3.7). The values obtained are shown in Table 6.4.

The pressure coefficient of the relative transit time for polysulfone is determined in a similar manner to that for the temperature coefficient. Each recorded waveform is fitted to the reference one, and the relative change of the transit time $(1 - \tau/\tau_0)$ for a given pressure is obtained. The results for the longitudinal and the shear waves are shown in Fig. 6.4 and Fig. 6.5 respectively. The values of the pressure coefficients κ_l and κ_t are also listed in Table 6.4. To determine the pressure coefficient of the velocity or the constant K_T, one needs to know the isothermal compressibility β_T, which can be calculated from the adiabatic bulk modulus as $\beta_T = \gamma/B_S$, where γ is obtained from the expression, $\gamma = 1 + \alpha^2 VTB_S/C_p$, by using (2.2.26) and (2.2.27).

By using Eqs. (5.3.8) and (5.3.9) the constants K_T and K_p are calculated from coefficients κ_l and η_l respectively. Then, by using Eq. (2.2.28), the nonlinearity parameter B/A is calculated. The values of B/A for three polymers are listed in Table 6.4. In Table 6.5, the two nonlinearity parameters, β_3 and B/A are compared. As shown in Eq. (2.2.16), theoretically β_3 is equal to $-(B/A + 2)$. The results from the two methods agree with each other within the experimental uncertainty.

TABLE 6.3

The Longitudinal and Shear Velocity

at 5MHz, 25°C, and Atmospheric Pressure for Three Polymers

	PMMA	Polystyrene	Polysulfone
c_l (m/sec)	2748.7 ± 0.6	2308.5 ± 0.7	2268.3 ± 0.8
c_t (m/sec)	1396.0 ± 1.1	1143.1 ± 1.9	945.7 ± 1.8
ζ*	1.969	2.020	2.399
σ†	0.326	0.338	0.395

* $\zeta \equiv c_l/c_t$, Eq.(5.3.12).

† Poisson's ratio $\sigma = (\zeta^2/2 - 1)/(\zeta^2 - 1)$

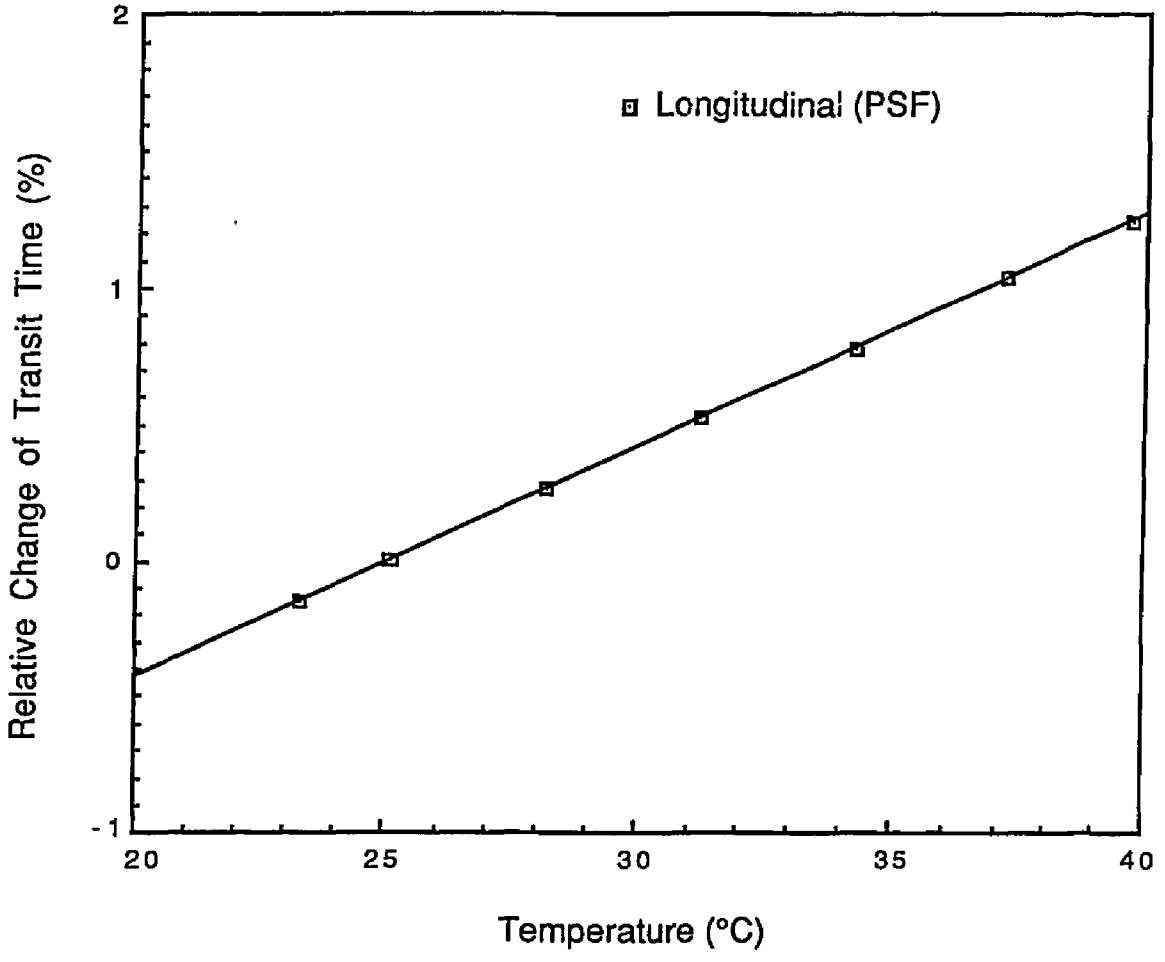

Fig. 6.2 The relative change in the longitudinal transit time, $(\tau/\tau_0 - 1)$ as a function of temperature for polysulfone at atmospheric pressure and 5 MHz.

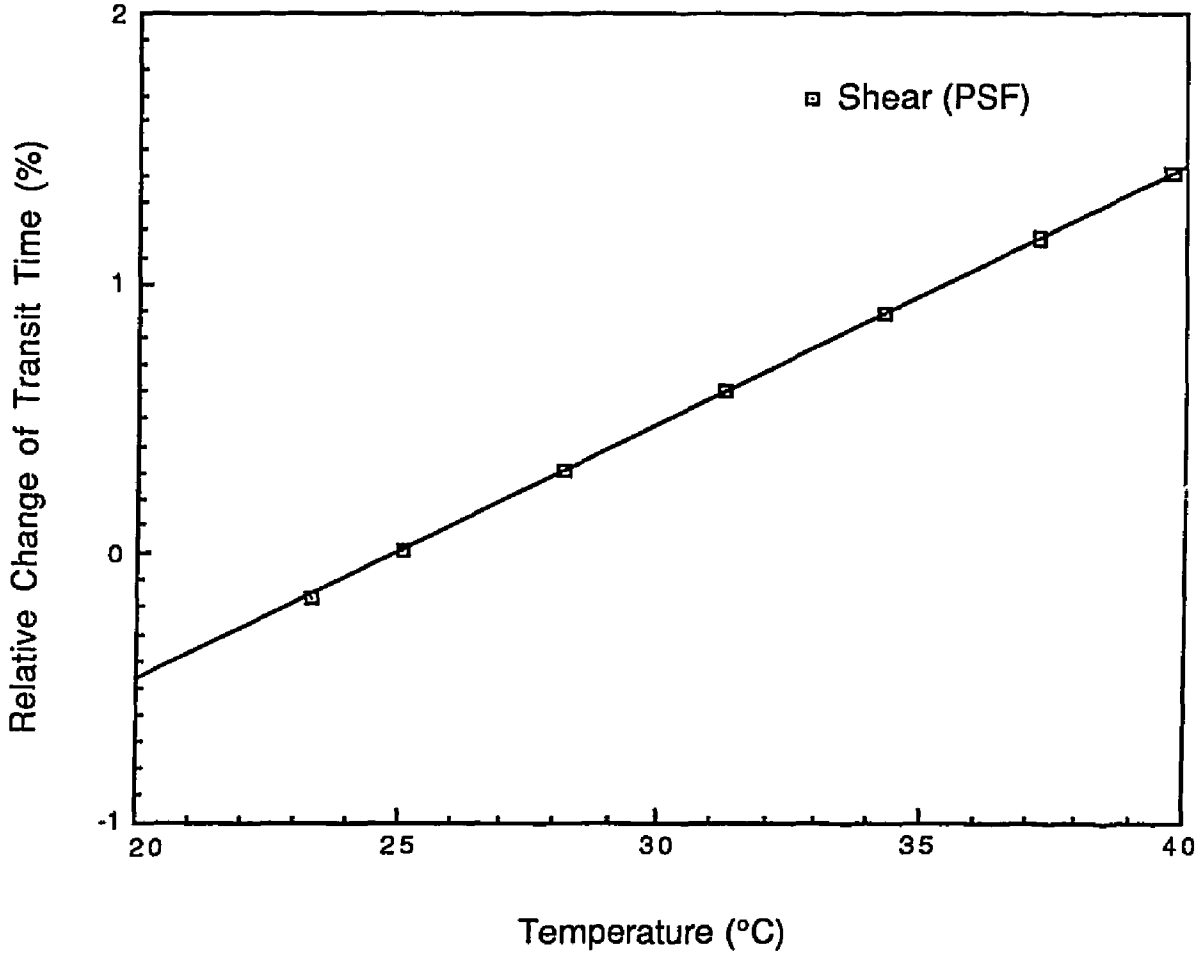

Fig. 6.3. The relative change in the shear transit time, $(\tau/\tau_0 - 1)$ as a function of temperature for polysulfone at atmospheric pressure and 5 MHz.

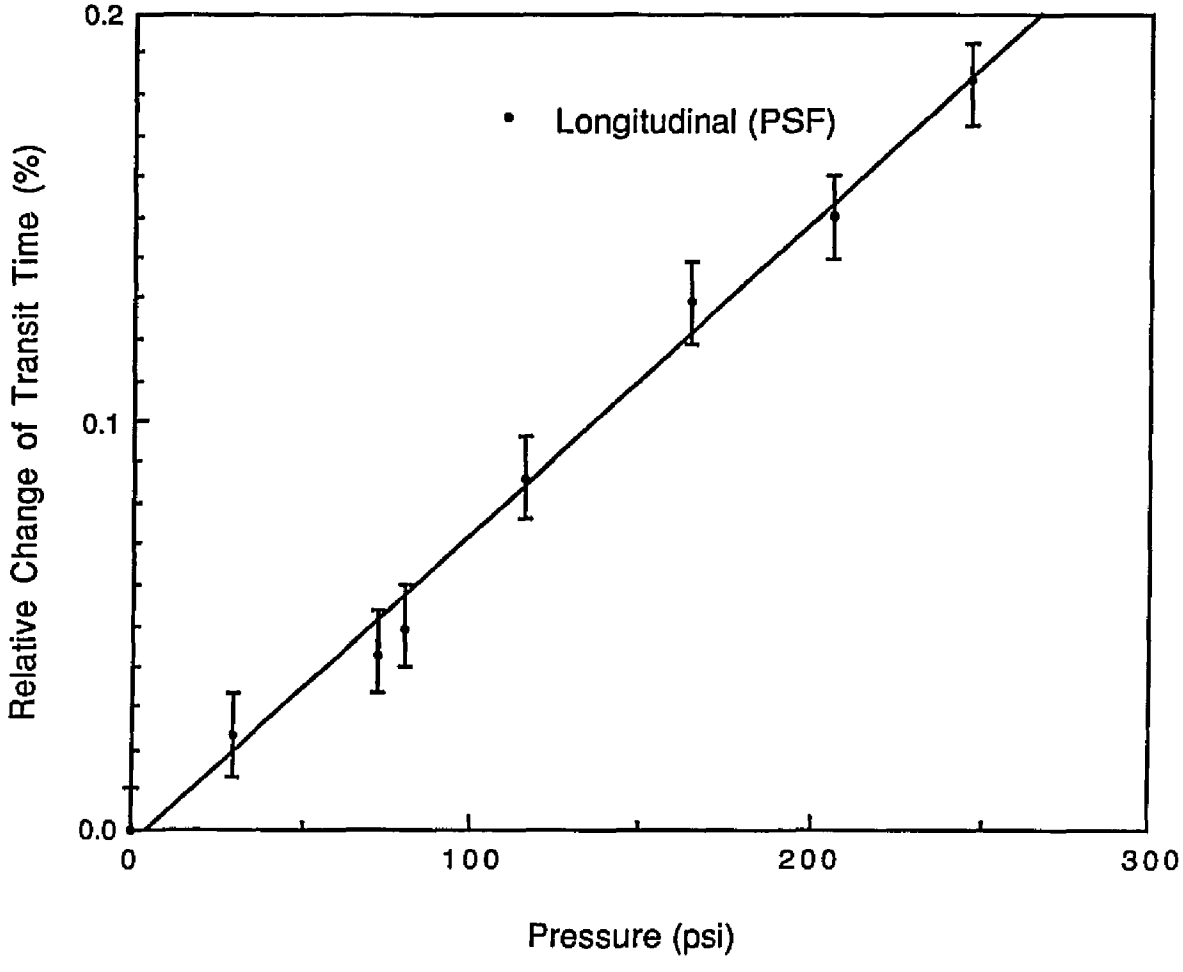

Fig. 6.4. The relative change in the longitudinal transit time, $(1 - \tau/\tau_0)$ as a function of pressure at 5MHz for polysulfone.

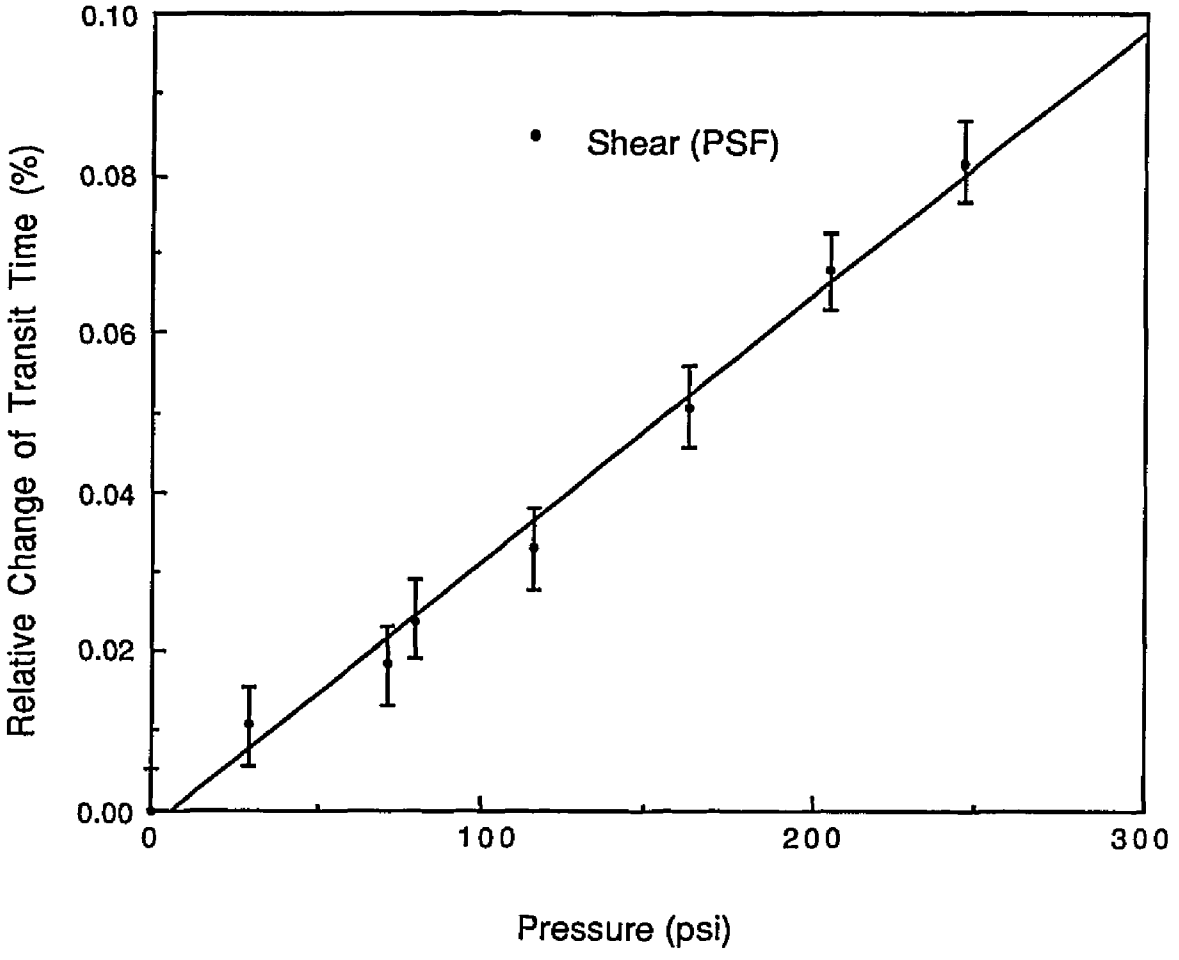

Fig. 6.5. The relative change in the shear transit time, $(1 - \tau/\tau_0)$ as a function of pressure at 5MHz for polysulfone.

TABLE 6.4

Acoustic and Thermal Constants of Three Polymers

	PMMA	PS	PSF
η_l (10^{-4}/°C)			8.497
η_t (10^{-4}/°C)			9.571
α (10^{-4}/°C)[1]	2.16	2.10	1.67
$\partial \ln c_l / \partial T$ (10^{-4}/°C)	-9.628[2]	-7.387[3]	-7.939
$\partial \ln c_t / \partial T$ (10^{-4}/°C)	-8.942[2]	-5.460[3]	-9.013
K_p	4.46	3.52	4.78
κ_l (10^{-10}/Pa)	9.652	11.10	10.98
κ_t (10^{-10}/Pa)	7.642	6.127	4.809
B_S (10^9Pa)	5.881	3.764	4.884
β_S (10^{-10}/Pa)	1.700	2.657	2.048
C_p (J/kg°C)	1420[4]	1225[4]	1130[1]
γ-1	0.0486	0.0385	0.0292
β_T (10^{-10}/Pa)	1.783	2.759	2.107
K_T	5.08	3.69	4.88
B/A	10.2	7.4	9.8

[1] [Plastics 1980]

[2] [Asay 1969]

[3] [Lamberson 1972]

[4] [Domalski 1984]

Table 6.5

Comparison of Nonlinearity Parameters β_3 and B/A for Three Polymers

	PMMA	PS	PSF
$-\beta_3$	13.3±0.7	11.1±0.8	10.9±0.6
B/A + 2	12.2±1.1*	9.4±1.0†	11.8±1.1#

*Calculated from the data in [Asay 1969].

†Calculated from the data in [Lamberson 1972].

#This work.

6.3 The Grüneisen parameters and the Interchain Specific Heat

The pressure coefficients of the transit time are used to calculate the acoustic Grüneisen parameter by using Eq. (5.3.13). First the average pressure coefficient, κ_s, is calculated from the longitudinal and shear pressure coefficients. The acoustic Grüneisen parameter, Γ_T, is then determined. For comparison, the thermodynamic Grüneisen parameter, Γ, is calculated from coefficient of thermal expansion, compressibility and specific heat by using Eq. (2.3.8). We find that Γ_T is about 4 to 6 times of Γ, as described in Section 2.3, which is typical for polymers. By using Eq. (2.3.8), the interchain specific heat for three polymers is then calculated and listed in Table 6.6.

Table 6.6

Grüneisen Parameters and Interchain Specific Heat of Three Polymers

	PMMA	PS	PSF
κ_S (10^{-10}/Pa)	7.766	6.412	5.025
Γ_T	4.36	2.32	2.38
Γ	0.754	0.615	0.584
Γ/Γ_T	0.173	0.265	0.245
$C_{V,i}$ (J/kg°C)	258	336	285

6.4 Discussion

We have related three types of nonlinearity parameters to each other. The parameter β_3 from harmonic generation and B/A from a stressed specimen are based on similar nonlinear equations. Similarly to B/A, the Grüneisen parameter, Γ_T, is determined from the pressured dependence of sound velocity; although the latter includes the contributions both from the longitudinal and shear modes. For polymers, all the nonlinearity parameters show larger values than those found for metals or ionic solids. (The three investigated polymers have values of β_3 which are greater than 10; while typical values for metals are in the neighborhood of 5.) The higher nonlinearity for polymers reflects the nature of the weaker interaction between the molecules. Moreover from a comparison of Grüneisen parameters, we find that the acoustic nonlinearity parameters for polymers seem to be dominated by the interchain interactions.

Some researchers have tried to construct a physical model which describes the relationship of the Grüneisen parameter to the intermolecular potential, based on the Lennard- Jones expression of the form $U = ar^{-n} - br^{-m}$, converted from particle-particle potential into chain-chain potential [Barker 1967]. However, it is found that Γ_T is very sensitive to the asymmetries in U and to the details of

its shape. The nonlinearity depends on the structure of the chains. For example, the existence of chain folds can affect the local potential and therefore the nonlinearity. The probability of the chain-fold formation at glass transition is significantly different for various polymers. It is strongly dependent on the polymer structure above the glass transition temperature T_g.

For amorphous polymers, a rubbery state exists above T_g. In the rubbery state, individual units, atomic group and segments undergo intensive thermal motion; but the rapid movement of the macromolecules as separate kinetic units is still impossible. Some of polymers in this state are capable of undergoing enormous recoverable deformation, which sometimes amount to several hundred percent [Perepechko 1978]. This phenomenon can be seen as the folded flexible long chains straighten out under applied stress and return to their original shape after the stress is removed, as a result of thermal motion. According to the kinetic theory of rubber elasticity, a polymer is not regarded as an assembly of individual chains, but rather as a sparse network [Treloar 1958]. The main characteristic of the network can be described by a parameter M_c, which is the average molecular mass of the chain element between two neighboring entanglement points of the network. According to this theory, the characteristic molecular mass M_c can be

estimated as $M_c = 3\rho RT/E \approx \rho RT/G$, where R is the universal gas constant, E the Young's modulus, and G the shear modulus. If M_0 denotes the molecular mass of the repeating unit then $N_c \equiv M_c/M_0$ is the number of units between two entanglement points [Porter 1966]. Obviously the characteristic number N_c indicates to an extent the rigidity of the skeleton structure of the network. The smaller the value of N_c, the stiffer the system is. For example, according to Perepechko's data [Perepechko 1976], the stiffest one among the three investigated polymers is polysulfone with a N_c = 2.4; while N_c = 33 for polystyrene, and N_c = 52 for PMMA. The data also show that polysulfone has the shear modulus G_0 of about 5MPa in the rubber-elastic plateau, whereas PMMA has only about 1MPa.

It is reasonable to expect that, for amorphous polymers, the larger the number N_c, the higher the probability of forming chain folds on the transition from a rubbery to a glassy state. A polymer with a smaller modulus in the rubbery plateau state tends to form, in the glassy state, ordered regions consisting of chain folds. In contrast, a rigider and denser entanglement network will prevent the polymer chains from being tightly packed in the glassy state. The result is the shear modulus of a polymer in the glassy state will typically decrease as the density of the entanglement network increases. This trend can be seen in

our room temperature ultrasonic data, with PSF having the smallest and PMMA the largest modulus.

Based on this supposition, it is naturally to relate the nonlinearity parameters to the chain structure. As shown in our results, PMMA has larger values of nonlinearity parameters, compared to the other two. A more tightly packed system with more chain folds might be more sensitive to the change of the spacing caused by external stimuli, such as applied stress, and therefore has greater nonlinearity. However, as considering the intermolecular potential, the real form of the potential should be even more complicated based on the foregoing assumption. The correlation between the nonlinearity parameter and the potential is not straightforward.

It is obvious that all the acoustic nonlinearity parameters for polymers are dominated by interchain interactions. While the details of the interaction are still obscure, these nonlinearity parameters may be basic tools for improving our understanding of the interactions in polymeric and other solids. This would be enhanced by measurements of these nonlinearity parameters in a more extensive range of temperature; particularly in the regions of transitions and other structure relaxation processes. Two methods for determining nonlinearity parameters are introduced in this work, one using contact transducers to measure

harmonic generation, the other measuring the pressure (or strain) dependence of sound velocity. They can be complementary for various experimental conditions; and, if coupled to thermal expansion and heat capacity measurements, the nonlinearity measurements will provide useful information for the understanding of various phenomena and properties of polymers.

In summary, in this research we have uncovered relationships between various types of nonlinearity parameters for solids. In addition, we have developed a new technique for quantitative measurements of nonlinearity of solids using contact transducers. The improvement to the conventional technique in sensitivity is significant. This new technique offers an attractive alternative. Moreover, the measurement of the nonlinearity provides a means of characterizing interchain interactions in polymer materials.

APPENDIX

LIST OF SYMBOLS

B_S	adiabatic bulk modulus
B_T	isothermal bulk modulus
B/A	nonlinearity parameter, ratio of B and A that is defined by Eqs. (2.2.12) and (2.2.13)
c	ultrasonic velocity
c_{ijkl}	adiabatic (isentropic) second-order elastic stiffness coefficients
c_s	average sound velocity for a Debye solid, see Eq. (2.3.2)
C	capacitance
C_p	specific heat at constant pressure
C_V	specific heat at constant volume
E	voltage
E	Young's modulus
F	stress
f	frequency
G	shear modulus, $G = \mu$
i	electric current
j	$\sqrt{-1}$

J	Jacobian, $J = \det[\partial y_i/\partial x_j]$
k	electromechanical coupling constant
K_p	the relative change of the ultrasonic velocity with respect to the volume change at constant pressure, defined by Eq. (2.2.24)
K_T	the relative change of the ultrasonic velocity with respect to the volume change at constant temperature, defined by Eq. (2.2.23)
l	length, thickness
$()_l$	subscript indicates the quantity associated with the longitudinal wave
M_i	linear combination of elastic coefficients of ith- and the lower order
p	pressure
p_l	longitudinal stress, see Eq. (2.3.3)
S	entropy
S	cross-sectional area
t	time
$()_t$	subscript indicates the quantity associated with the shear wave
T	temperature
T_{ij}	stress tensor
u	particle displacement
u_{ij}	strain tensor
v	particle velocity
V	volume, specific volume

x_i Lagrangian coordinate

y_i position of a particle in an arbitrary configuration, $y_i = x_i + u_i$

Z impedance

α volume coefficient of thermal expansion

α_1 attenuation coefficient of the fundamental wave

α_2 attenuation coefficient of the second harmonic

β_S adiabatic compressibility

β_T isothermal compressibility

β_3 nonlinearity parameter, $\beta_3 \equiv M_3/M_2$

γ ratio of C_p/C_V

Γ thermodynamic Grüneisen parameter, defined by Eq. (2.3.7)

Γ_T acoustic Grüneisen parameter, defined by Eq. (2.3.6b)

δ difference of two attenuation coefficients, $\delta \equiv 2\alpha_1 - \alpha_2$

δ_{ij} unit tensor

ε electric permittivity

η temperature coefficient of ultrasonic transit time, see Eqs. (5.3.3) and (5.3.4)

κ pressure coefficient of the transit time, see Eqs. (5.3.1) and (5.3.2)

κ_s average pressure coefficient of the transit time, see Eq. (5.3.11)

λ wavelength

μ one of Lamé constants; $\mu = G$, shear modulus

ρ density

σ Poisson's ratio

τ ultrasonic transit time, $\tau = l/c$

ω angular frequency

ω_D Debye frequency

ξ the condensation, $\xi \equiv (\rho - \rho_0)/\rho_0$, (2.2.11)

ζ ratio of the longitudinal velocity to the shear velocity, $\zeta = c_l/c_t$

REFERENCES

Allen, G., J. McAinsh, and G. M. Jeffs, Polymer 12, 85 (1971)

Asay, J. R., D. L. Lamberson, and A. H. Guenther, J. Appl. Phys. 40, 1768 (1969).

Ashcroft, N. W. and N. D. Mermin, *Solid State Physics* (Holt, Rinehart and Winston, New York, 1976), pp. 488-509.

Barker, R. E., Jr., J. Appl. Phys. 38, 4234 (1967).

Berlincourt, D. A., D. R. Curran, and H. Jaffe, in *Physical Acoustics* Vol. 1A, ed. by W. P. Mason (Academic Press, New.York, 1964), Ch. 3, pp. 169-270.

Beyer, R. T., in *Physical Acoustics*, Vol. 2-B, ed. by W. P. Mason (Academic Press, New York, 1965), Ch. 10, pp. 231-264.

Breazeale, M. A., J. H. Cantrell, Jr., and J. S. Heyman, in *Methods of Experimental Physics*, Vol. 19, ed. by P. D. Edmonds (Academic Press, New York, 1981), Ch. 2, pp. 67-135.

Desilets, M. A., J. D. Fraser, and G. S. Kino, IEEE Trans. Sonics and Ultrasonics, SU-25, 115 (1978).

Domalski, E. S., W. H. Evans, and E. D. Hearing, *Heat Capacities and Entropies of Organic Compound in the Condensed*

Phase (J. Phys. Chem. Ref. Data, V. 13, Suppl. no. 1) (ACS and AIP, Washington and New York, 1984).

Gauster, W. B. and M. A. Breazeale, Rev. Sci. Instr. 37, 1544 (1966).

Hartmann, B. and J. Jarzynski, J. Appl. Phys. 43, 4304 (1972).

Hartmann, B., Acustica 36, 24 (1976/77).

Khimunin, A. S., Acustica, 27, 173 (1972).

Lamberson, D. L., J. R. Asay, and A. H. Guenther, J. Appl. Phys. 43, 976 (1972).

Landau, L. D. and E. M. Lifshitz, *Theory of Elasticity* (Pergamon Press, London, 1959), p. 11.

Leedom, D. A., R. Krimholtz, and G. L. Matthaei, IEEE Trans. Sonics and Ultrasonics, SU-18, 128 (1971).

Li, K. P., Ph.D. dissertation, College of William and Mary (1984).

Papadakis, E. P., in *Physical Acoustics*, Vol. 12, ed. by W. P. Mason and R. N. Thurston (Academic Press, New York, 1976), Ch. 5, pp. 277-374.

Parker, F. R., W. P. Winfree, and M.-C. Wu, IEEE 1986 Ultrasonics Symposium Proceedings, 1009 (1986).

Perepechko, I. I., *An Introduction to Polymer Physics* (Mir, Moscow, 1978; English Transl., 1981).

Perepechko, I. I. and O. V. Startsev, Sov. Phys. Acoust. 22, 419 (1976).

Phillips, D. W., A. M. North, and R. A. Pethrick, J. Appl.

Polym. Sci. 21, 1859 (1977).

Plastics/*A Desk-top Data Bank, Edition 5, Book B* (The International Plastics Selector, Inc., San Diego, 1980).

Porter, R. S. and J. F. Johnson, Chem. Rev. 66, 1 (1966).

Reif, F., *Fundamentals of Statistical and Thermal Physics* (McGraw-Hill, New York, 1965), pp. 411-418.

Sittig, E. K., IEEE Trans. Sonics and Ultrasonics, SU-14, 167 (1967).

Sittig, E. K., IEEE Trans. Sonics and Ultrasonics, SU-16, 2 (1969).

Slater, J. C., *Introduction to Chemical Physics* (McGraw-Hill, New York, 1939; Dover, New York, 1970), p. 219.

Smith, R. T. and F. S. Welsh, J. Appl. Phys. 42, 2219 (1971).

Swan, P. R., J. Polym. Sci. 56, 403 (1962).

Thompson, R. B. and H. F. Tiersten, J. Acoust. Soc. Am. 62, 33 (1977).

Thurston, R. N. and M. J. Shapiro, J. Acoust. Soc. Am. 41, 1112 (1967).

Treloar, L. R. G., *The Physics of Rubber Elasticity* (Clarendon, Oxford, 1958), pp. 44-84.

Wada, Y., A. Itani, T. Nishi, J. Polym. Sci. A-2 7, 201 (1969).

Wallace, D. C., in *Solid State Physics*, Vol. 25, ed. by H. Ehrenreich, F. Seitz, and D. Turnbull (Academic Press, New York, 1970), p. 301

Warfield, R. W., Makromol. Chem. 175, 3285 (1974).

Warner, A. W., M. Onoe, and G. A. Coquin, J. Acoust. Soc. Am. 42, 1223 (1967).

Wu, M.-C. and W. P. Winfree, IEEE 1987 Ultrasonics Symposium Proceedings, 1147 (1987).

VITA

Meng-Chou Wu

- Born in Juifang, Taipei, Taiwan, August 10, 1951.
- Graduated from The Affiliated High School of Taiwan Normal University, Taipei, 1969.
- B.S., National Cheng-Kung University in Taiwan, 1974.
- A teacher at Nan-Ning Middle School, Tainan, Taiwan, 1976-1978.
- M.S., National Cheng-Kung University in Taiwan, 1980, with a concentration in particle physics.
- A lecturer of physics at Fu-Jen Catholic University in Taiwan, 1980-1983.
- In July 1983, he entered the College of William and Mary as a graduate assistant in the Department of Physics.
- Joined the NMR group of the Department, working with Dr. M. S. Conradi on molecular solids, 1984-1986.
- Joined the ultrasonics group at NASA Langley Research Center, working with Dr. J. S. Heyman and Dr. W. P. Winfree, on polymeric solids, 1986-1989.